





This is to certify that the  
thesis entitled

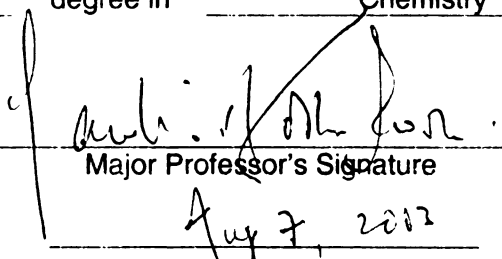
**SYNTHESIS AND CHARACTERIZATION OF NEW  
POLYETHER-BASED ADVANCED MATERIALS**

presented by

Yuqing Chen

has been accepted towards fulfillment  
of the requirements for the

M.S. degree in Chemistry

A handwritten signature in dark ink, appearing to read "Paul J. H. Lee", is written over a horizontal line. The signature is stylized and cursive.

Major Professor's Signature

Aug 7, 2012

Date

PLACE IN RETURN BOX to remove this checkout from your record.  
TO AVOID FINES return on or before date due.  
MAY BE RECALLED with earlier due date if requested.

DATE DUE	DATE DUE	DATE DUE
NOV 14 2006		

**SYNTHESIS AND CHARACTERIZATION OF  
NEW POLYETHER-BASED ADVANCED MATERIALS**

By

Yuqing Chen

A THESIS

Submitted to  
Michigan State University  
in partial fulfillment of the requirements  
for the degree of

MASTER OF SCIENCE

Department of Chemistry

2003



## **ABSTRACT**

### **SYNTHESIS AND CHARACTERIZATION OF NEW POLYETHER-BASED ADVANCED MATERIALS**

By

Yuqing Chen

In recent years, electroconducting organic polymers have become very promising materials because of their numerous technological applications. These include antistatic and magnetic coating, sensors and actuators, batteries and modified electrodes. The major focus of this project is the design, synthesis and characterization of polymers with the potential for having useful and unique electrical and magnetic properties together with attractive processibility and mechanical characteristics. We explored the use of certain dense polyether compounds or macromolecular scaffolds with functionalities that facilitate charge transfer where fixed ions form a dense matrix in which mobile counter-ions or electrons move. The systems are nominally polymeric in nature and contain functionalities that capture or solvate the appropriate ions or charged species. Certain groups, such as pentafluorobenzyl and nitrobenzoyl groups, are strong electron acceptors and they play the role of 'electron sponge' in the material. We prepared several such systems which upon doping by strong electron donors like Na or K produced new materials that exhibit very interesting and important spectroscopic, magnetic and electronic properties.

## ACKNOWLEDGEMENTS

I would like to express my sincere gratitude to my research advisor, Dr. Rawle I. Hollingsworth, for his guidance, encouragement and support throughout my graduate study in Chemistry at Michigan State University. I would also like to thank Dr. Jack Throck Watson and Dr. Jetze J. Tepe for serving on my guidance committee and giving me valuable suggestions to my thesis.

My deepest thanks go to my husband, Donghui Zhang, and my parents for their endless love, understanding and continuous support that make my life enjoyable.

I am also grateful to all Hollingsworth group members for their friendship and collaboration.

## TABLE OF CONTENTS

List of Schemes.....	viii
List of Figures.....	ix
List of Tables.....	xii
 <b>Chapter 1. Background.....</b>	 <b>1</b>
1.1. Electro-Active Polymeric Materials.....	2
1.1.1. Introduction.....	2
1.1.2. Electronically Conductive Polymers.....	2
1.1.3. Ionically Conductive Polymers.....	7
1.2. Magnetochemistry.....	10
1.2.1. Classes of Magnetic Materials.....	10
1.2.2. Molecule-Based Magnets.....	19
1.2.3. Magnetic Conductors.....	20
1.3. References.....	22
 <b>Chapter 2. Solvated Electrons, Electrides and Alkalides.....</b>	 <b>24</b>
2.1. Solvated Electrons.....	25
2.1.1. Introduction.....	25
2.1.2. Methods of Producing Solvated Electrons.....	25
2.1.3. Properties of Solvated Electrons.....	28
2.2. Electrides and Alkalides.....	32

2.2.1. Introduction.....	32
2.2.2. Crystalline Alkalides.....	33
2.2.3. Electrides Properties.....	34
2.2.4. Future Directions.....	35
2.3. References.....	37

### **Chapter 3. Design. Synthesis and Characterization of the Doped Poly(glycidyl**

<b>pentafluorophenyl ether).....</b>	<b>39</b>
3.1. Rationale Design and Structure.....	40
3.1.1. Hexafluorobenzene Radical Anion.....	40
3.1.2. Structure of the Doped Poly(glycidyl pentafluorophenyl ether).....	41
3.2. Experimental.....	48
3.2.1. Synthesis of Poly(glycidyl pentafluorophenyl ether).....	48
3.2.2. Doping.....	51
3.2.3. Characterization of the Materials.....	51
3.2.3.1. Gel Permeation Chromatography.....	51
3.2.3.2. FT-IR Spectroscopy.....	51
3.2.3.3. NMR Spectroscopy.....	52
3.2.3.4. UV-visible Spectroscopy.....	52
3.2.3.5. SQUID Measurements.....	52
3.2.3.6. Conductivity Measurements.....	53
3.2.3.7. EPR spectroscopy.....	53
3.3. Results and Discussion.....	54

3.3.1. Synthesis of Poly(glycidyl pentafluorophenyl ether).....	54
3.3.1.1. Preparation of Glycidyl Pentafluorophenyl Ether.....	54
3.3.1.2. Polymerization of Glycidyl Pentafluorophenyl Ether.....	55
3.3.2. Characterization of Poly(glycidyl pentafluorophenyl ether).....	57
3.3.2.1. Solubility.....	57
3.3.2.2. GPC Results.....	57
3.3.3. Characterization of the Doped Poly(glycidyl pentafluorophenyl ether).....	59
3.3.3.1. UV-visible Spectra.....	59
3.3.3.2. Magnetic Properties.....	65
3.3.3.3. Conductivity Measurements.....	75
3.3.3.4. EPR Analysis.....	76
3.4. References.....	79
3.5. Conclusions.....	81

<b>Chapter 4. Synthesis and Characterization of the Doped Poly[penta(ethylene glycol) dinitrobenzoyl ether] and Poly[penta(ethylene glycol) pentafluorophenyl ether].....</b>	<b>82</b>
4.1. Experimental.....	83
4.1.1. Synthesis of Poly[penta(ethylene glycol) dinitrobenzoyl ether].....	83
4.1.2. Synthesis of Poly[penta(ethylene glycol) pentafluorophenyl ether].....	86
4.1.3. Doping.....	89
4.2. Results and Discussion.....	90
4.2.1. Characterization of the Undoped Polymers.....	90

4.2.1.1. Solubility.....	90
4.2.1.2. GPC Results.....	90
4.2.2. Characterization of the Doped Polymers.....	94
4.2.2.1. UV-visible Spectra.....	94
4.2.2.2. Magnetic Properties.....	95
4.2.2.3. EPR Analysis.....	98
4.4. References.....	100
<b>Appendices.....</b>	<b>101</b>
<b>Appendix 1 - <math>^1\text{H}</math>-NMR spectrum of glycidyl pentafluorophenyl ether.....</b>	<b>102</b>
<b>Appendix 2 - <math>^{13}\text{C}</math>-NMR spectrum of glycidyl pentafluorophenyl ether.....</b>	<b>103</b>
<b>Appendix 3 - <math>^{19}\text{F}</math>-NMR spectrum of glycidyl pentafluorophenyl ether.....</b>	<b>104</b>
<b>Appendix 4 - <math>^1\text{H}</math>-NMR spectrum of poly(glycidyl pentafluorophenyl ether).....</b>	<b>105</b>

## LIST OF SCHEMES

Scheme 3.1. Synthesis of poly(glycidyl pentafluorophenyl ether).....	48
Scheme 4.1. Synthesis of poly[penta(ethylene glycol) dinitrobenzoyl ether].....	84
Scheme 4.2. Synthesis of poly[penta(ethylene glycol) pentafluorophenyl ether].....	87

## LIST OF FIGURES

Images in this thesis are presented in color.

Figure 1.1. Molecular structures of examples of conjugated polymers.....	5
Figure 1.2. Conductivity of electronic polymers.....	6
Figure 1.3. Diamagnetism. (a) Magnetization as a function of magnetic field. (b)	
Magnetic susceptibility as a function of temperature.....	11
Figure 1.4. Paramagnet disordered spins.....	12
Figure 1.5. Paramagnetism. (a) Magnetization as a function of magnetic field. (b)	
Magnetic susceptibility as a function of temperature.....	12
Figure 1.6. Paramagnetism showing Curie and Curie-Weiss laws.....	13
Figure 1.7. Parallel alignment of spins in ferromagnetic materials.....	15
Figure 1.8. Typical hysteresis loop for an ordered ferro- or ferrimagnet.....	16
Figure 1.9. Magnetic susceptibility vs. temperature curve for ferromagnetic and	
paramagnetic materials.....	17
Figure 1.10. Antiparallel alignment of spins in ferrimagnetic materials.....	17
Figure 1.11. Antiparallel alignment of spins in antiferromagnetic materials.....	18
Figure 1.12. Magnetic susceptibility vs. temperature curve for antiferromagnetic	
materials.....	19
Figure 3.1. The structure of poly(glycidyl pentafluorophenyl ether).....	44



Figure 3.2. Molecular electrostatic potential surface for (a) methylpentafluorophenyl ether and (b) methylpentafluorophenyl ether radical anion calculated using PM3 semi-empirical method.....	47
Figure 3.3. GPC chromatogram of (a) Polystyrene standards (b) Poly(glycidyl pentafluorophenyl ether).....	58
Figure 3.4. lg MW v.s. $K_{av}$ standard curve for poly(glycidyl pentafluorophenyl ether)...	58
Figure 3.5. Solution of the alkali metal-doped poly(glycidyl pentafluorophenyl ether) in THF.....	60
Figure 3.6. UV-vis absorption spectra of the doped poly(glycidyl pentafluorophenyl ether).....	61
Figure 3.7. UV-vis spectra of (a) hexafluorobenzene radical anion and (b) methoxypentafluorobenzene radical anion from Zindo calculations.....	63
Figure 3.8. Magnetic properties of high MW poly(glycidyl pentafluorophenyl ether) doped with 20 wt % potassium.....	69
Figure 3.9. Magnetic properties of high MW poly(glycidyl pentafluorophenyl ether) doped with 30 wt % sodium.....	70
Figure 3.10. Magnetic properties of high MW poly(glycidyl pentafluorophenyl ether) doped with 22 wt % sodium.....	72
Figure 3.11. Magnetic properties of medium MW poly(glycidyl pentafluorophenyl ether) doped with 25 wt % potassium.....	73
Figure 3.12. Magnetic properties of medium MW poly(glycidyl pentafluorophenyl ether) doped with 35 wt % sodium.....	74

Figure 3.13. EPR spectra of high MW poly(glycidyl pentafluorophenyl ether) doped with 40 wt % potassium at different temperatures.....	78
Figure 4.1. GPC chromatogram of (a) Polystyrene standards (b) Poly[penta(ethylene glycol) dinitrobenzoyl ether].....	92
Figure 4.2. lg MW v.s. $K_{av}$ standard curve for poly[penta(ethylene glycol) dinitrobenzoyl ether].....	92
Figure 4.3. GPC chromatogram of (a) Polystyrene standards (b) Poly[penta(ethylene glycol) pentafluorophenyl ether].....	93
Figure 4.4. lg MW v.s. $K_{av}$ standard curve for poly[penta(ethylene glycol) pentafluorophenyl ether].....	93
Figure 4.5. UV-vis absorption spectra of the doped poly[penta(ethylene glycol) dinitrobenzoyl ether] and poly[penta(ethylene glycol) pentafluorophenyl ether].....	94
Figure 4.6. Magnetic properties of poly[penta(ethylene glycol) dinitrobenzoyl ether] doped with 30 wt % potassium.....	96
Figure 4.7. Magnetic properties of poly[penta(ethylene glycol) pentafluorophenyl ether] doped with 0.5 wt % potassium.....	97
Figure 4.8. EPR spectra of poly[penta(ethylene glycol) dinitrobenzoyl ether] doped with 20 wt % potassium at different temperatures.....	99
Figure 4.9. EPR spectra of poly[penta(ethylene glycol) pentafluorophenyl ether] doped with 10 wt % potassium at different temperatures.....	100

## LIST OF TABLES

Table 3.1. Polymerization of glycidyl pentafluorophenyl ether with antimony (V) chloride or potassium t-butoxide.....	56
Table 3.2. The room-temperature dc electrical resistance of doped poly(glycidyl pentafluorophenyl ether) in THF.....	75

## **Chapter 1. Background**

## **1.1. Electro-Active Polymeric Materials**

### **1.1.1. Introduction**

Electro-active polymeric materials are used today as sensors and biosensors, for corrosion protection coatings, for transistors, capacitors, and light emitting devices, for microactuators, microelectronic devices, and Shotky barriers, as well as electrochromic displays, catalysts, functional membranes and so on. There is also growing interest in using them as nanowires, for rechargeable batteries and energy storage, for photoelectrodes and antistatic coatings, dissipation of spacecraft charging, printed board surface finish, etc. Among these materials, two groups of electro-active polymers can be distinguished: i) electronically conductive polymers, which have conjugated bonds in a macromolecule, such as polyaniline, PANI. ii) ionically conductive polymers (polymeric ion conductors; polymer electrolytes), where the electrical signal is transported by ions weakly coordinated to a polymer, such as poly(ethylene oxide), PEO.

### **1.1.2. Electronically Conductive Polymers**

It has been known for more than 40 years that the electric conductivity of the conjugated polymer chains is by orders of magnitude higher than that of other polymeric materials.<sup>1</sup> In conjugated polymers, the chemical bonding leads to one unpaired electron (the  $\pi$ -electron) per carbon atom. Moreover,  $\pi$ -bonding, in which the carbon orbitals are in the  $sp_2p_z$  configuration and in which the orbitals of successive carbon atoms along the

backbone overlap, leads to electron delocalization along the backbone of the polymer. This electron delocalization provides the “highway” for charge mobility of the polymer chain. Such polymers can exhibit semiconducting or even metallic properties. Figure 1.1 shows some classic examples of conjugated polymers. Note the bond-alternated structures.

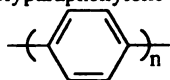
In 1974, Shirakawa and coworkers<sup>2</sup> discovered that the electronic conductance of polyacetylene maybe further increased by many orders of magnitude by “doping it” with electron acceptors (p-type dopants) such as iodine. In 1977, the rediscovery of this phenomenon by MacDiarmid and coworkers<sup>3</sup> triggered the explosive growth of research in the field of conductive polymers. A year later<sup>4</sup> it was discovered that analogous effects may also be induced by electron donors (n-type dopants). A term “intrinsically conducting polymer (ICP)” is used to describe such polymers that possess the electrical, electronic, magnetic, and optical properties of a metal while retaining the mechanical properties and processibility commonly associated with conventional polymers. More general terms are “synthetic metals” or “organic metals”. Figure 1.2 illustrates the increases in electrical conductivity of many orders of magnitude which can be obtained by doping. The conductivity attainable by an electronic polymer has very recently been increased an infinite number of times by the discovery of superconductivity in regioregular poly(3-hexylthiophene)<sup>5</sup>. Although this phenomenon was present only in a very thin layer of the polymer in a field effect (FET) configuration at a very low temperature (~2 K) it represents an historical quantum leap — superconductivity in an organic polymer.

Development of the intrinsically conducting polymers had actually been preceded by polymer composites which are merely a physical mixture of an insulating polymer with electrically conductive particles distributed throughout the material (conducting filled polymers). Conductive carbon blacks, short graphite fibers, metal coated glass fibers, as well as small metal particles or flakes have been used to introduce conductivity in such composites.<sup>6</sup> Their conductivity increases suddenly at a percolation threshold, at which the conductive phase dispersed in the non-conductive matrix becomes continuous. Their conductivity above percolation threshold could be as high as 0.5-0.1 S/cm, at 10-40 weight % fractions of the conductive filler. Size and shape of the particles strongly affects the position of the percolation threshold. The dominant use of filled polymers in electronic devices can be attributed to their ease of processing and wide range of electrical properties. Being inhomogeneous is an inherent weakness of filled polymer systems, which have three phases, namely the polymer, the filler, and the interface. Such inhomogeneity tends to result in problems such as lack of reproducibility, heavy process dependency, steep percolation threshold in conductivity, or weak dielectric strength. Controlling the quality of filler dispersion in a polymer matrix is the most critical and challenging technical issue in filled polymers.<sup>7</sup>

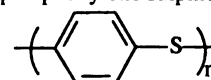
Polyacetylene (PA)



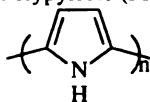
Polyparaphenylene (PPP)



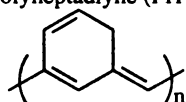
Polyparaphenylene sulphide (PPS)



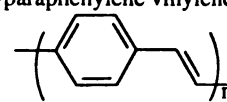
Polypyrrole (PPy)



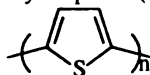
Polyheptadiyne (PHT)



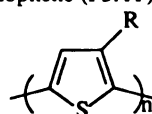
Polyparaphenylene vinylene (PPV)



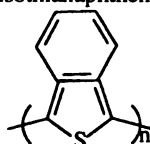
Polythiophene (PT)



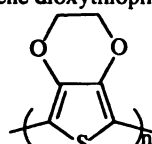
Poly (3-alkyl) thiophene (P3AT) (R-methyl, butyl, etc.)



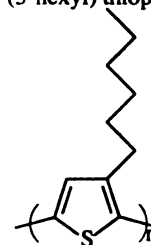
Polyisothianaphthene (PITN)



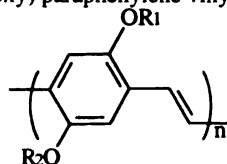
Polyethylene dioxythiophene (PEDOT)



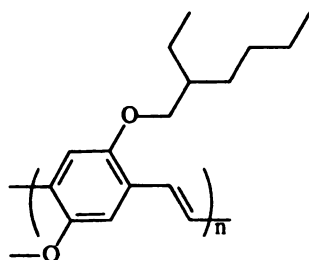
Poly (3-hexyl) thiophene (P3HT)



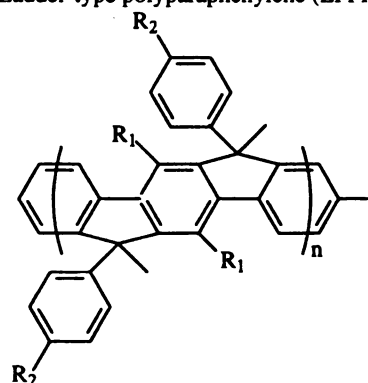
Poly (2,5-dialkoxy) paraphenylene vinylene (e.g. MEH-PPV)



Alkoxy-substituted poly para-phenylene vinylene (MEH-PPV)



Ladder-type polyparaphenylene (LPPP)



Polyaniline (PANI)

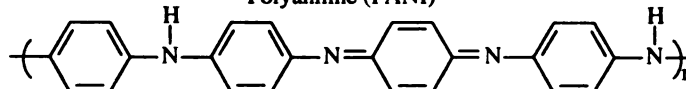


**Figure 1.1.** Molecular structures of examples of conjugated polymers.



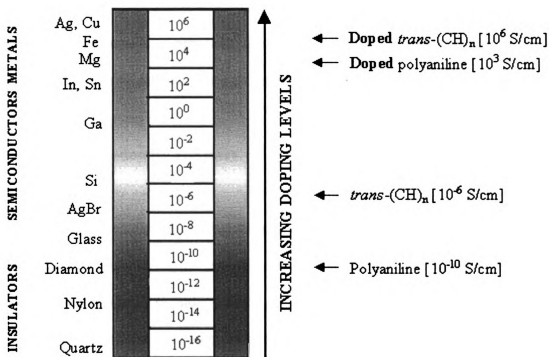


**Figure 1.2.** Conductivity of electronic polymers.

The very low density of polymers as compared to that of metals attracted the attention of the first investigators looking for possible applications of the newly discovered electrically conductive polymeric materials. However, poor stability limited their applicability in batteries and energy storage devices. Stability problems were solved with the discovery of the very stable polyaniline (PANI) and its analogues. Doped polypyrrole (PPy), polythiophene (PT) and their derivatives also seem to be quite stable, they are sensitive to oxygen only in their neutral form. Moreover, the newly discovered materials have properties that make them suitable for a great number of applications.

The initial conducting polymer systems were insoluble, intractable, and non-melting (and thus not processible) with relatively poor mechanical properties. In order to impart processibility and improve their mechanical characteristics, composites as well as

blends and grafts of the inherently conductive polymers into/with a non-conductive polymeric material have been prepared.<sup>8</sup> Equally important is the wide range of electrical conductivity that can be achieved through polymer blends.<sup>9</sup>

### **1.1.3. Ionically Conductive Polymers**

In recent years, the ionically conductive polymers, a related field of electronically conductive polymers, also explosively expanded. Progress in this area has been marked by an improvement in the understanding of salt-matrix interactions in polymer-salt complexes. M.B. Armand attributed the high cation mobility in polymer-salt complexes to the charge delocalization in the anion and the segment mobility in the polymer matrix. At the 4<sup>th</sup> European Polymer Federation Symposium, he presented new lithium salts of trifluoromethanesulfimide anions where high ion conductivities can be achieved because both the counter ion condensation is minimized and the softening effect occurs.<sup>10</sup> The chemical and thermal stability of polyelectrolytes has been improved by J.R. Reynolds et al. who used polybenzimidazole as a basis for the production of water-soluble electrolytes through the introduction of sulfonated side groups. As the polybenzimidazole chain is relatively stiff, thus contradicting one of Armand's criteria for good ion conduction.<sup>11</sup>

Polymer electrolytes are the subject of intensive study, in part because of their potential use as the electrolyte in all-solid-state rechargeable lithium batteries.<sup>12</sup> These materials are formed by dissolving a salt in a solid host polymer. Polymers such as PEO having flexible chains involving  $-\text{CH}_2\text{CH}_2-\text{O}-$  coordinative units can act as solvents of

metal salts, giving solid solutions, so-called polymer electrolytes, with ion conductivity values ranging from  $10^{-4}$  to  $10^{-5}$  S/cm at moderate temperatures ( $< 100^{\circ}\text{C}$ ). In certain cases crystalline complexes are formed by coordination of these oxyethylene units with alkali-metal ions, but the conductivity behavior has long been viewed as related to the amorphous fraction rather than to crystalline phases of the polymeric system.<sup>13</sup>

Ion transport in solids involves the hopping of ions between adjacent sites. In the conventional view of ionic conductivity in polymer electrolytes, ions move in a dynamic, disordered environment created by the polymer chain motion in the amorphous phase above the glass transition temperature,  $T_g$ . A crankshaft-like motion associated with short segments of the polymer chains randomly creates suitable coordination sites adjacent to ions so that these ions may then migrate. Such segmental modes involve the motion of groups of atoms on the polymer chains and are usually slow, limiting the migration rate of ions and therefore the maximum conductivity. Despite strenuous efforts over 20 years, the maximum conductivity of amorphous polymer electrolytes at room temperature remains around  $10^{-4}$  S/cm.<sup>14</sup>

Crystalline polymer electrolytes have received relatively little attention because they were not considered to support ionic conductivity. Zlatka Gadjourova and coworkers carried out an extensive study of the structural chemistry of crystalline polymer electrolytes and show that, in contrast to the prevailing view, ionic conductivity in the static, ordered environment of the crystalline phase can be greater than that in the equivalent amorphous material above  $T_g$ .<sup>14</sup> If the sites to which an ion migrates are already present in the polymer electrolyte owing to its structure, then as soon as the vibrating ion gains sufficient energy to hop, migration will take place. This may be

achieved by forming liquid crystalline polymer electrolytes designed with every pathway being identical and possessing bottlenecks of appropriate size for transport. Further support for the view that ion transport will be favored in crystalline polymer electrolytes comes from some crystalline ceramic materials such as  $\text{RbAg}_4\text{I}_5$  and  $\text{Li}_{0.5}\text{La}_{0.5}\text{TiO}_3$  which show ionic conductivities amongst the highest known in the solid state, exceeding by 1 to 3 orders of magnitude the maximum conductivity of conventional amorphous polymer electrolytes.<sup>15,16</sup> High ionic conductivity may also be obtained in plastic crystals where ion transport is aided by rotational disorder.<sup>17</sup> These results define a different direction in the search for ionically conducting polymers.

## **1.2. Magnetochemistry**

### **1.2.1. Classes of Magnetic Materials**

Magnetochemistry is the study of the magnetic properties of materials. The origin of magnetism lies in the orbital and spin motions of electrons and how the electrons interact with one another. In matter, the greatest magnetic effects are due to the spins of electrons rather than their orbital moments. The orbital moments play a part as well, but when there are uncompensated spins present in a molecule, the orbital contribution is overwhelmed.

There are different types of magnetism in materials. The various possible cases are called magnetic states of matter.

#### **(I). Diamagnetism**

Diamagnetism is part of all magnetic states but is usually negligible compared with other types of magnetism. A diamagnetic compound has all of its electron spins paired giving a net spin of zero. The origin of the magnetic moment is the orbit of the electrons around the nucleus. When Diamagnetic compounds are exposed to a field (H), an extra torque is applied to the electron, resulting in an antiparallel alignment of the atomic magnetic moment, therefore diamagnetic materials are weakly repelled by the magnet and a negative magnetization (M) and negative susceptibility ( $\chi$ ) are produced.

Another characteristic behavior of diamagnetic materials is that the susceptibility is temperature independent. See Figure 1.3.

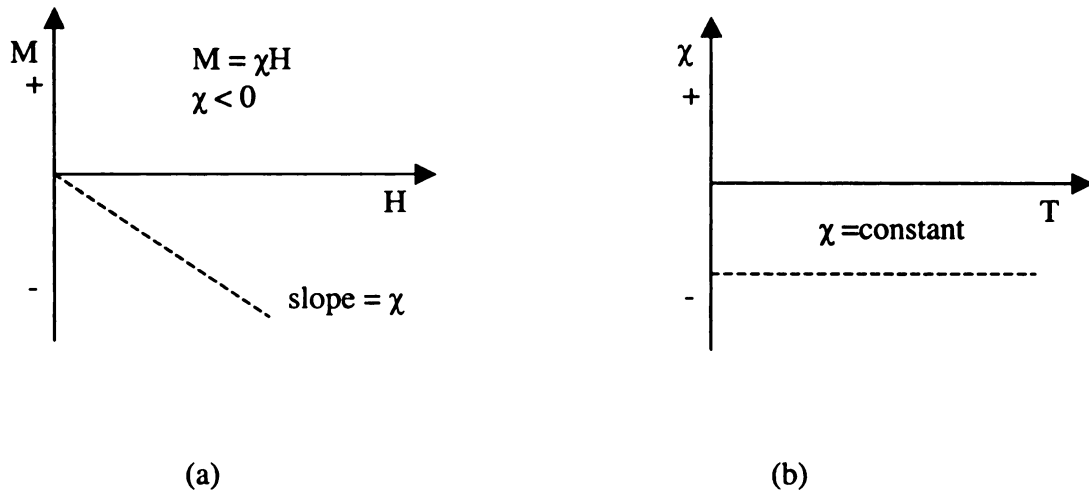


**Figure 1.3.** Diamagnetism. (a) Magnetization as a function of magnetic field. (b) Magnetic susceptibility as a function of temperature.

## (II). Paramagnetism

Paramagnetic materials are those in which individual atoms, ions or molecules have a permanent net spin magnetic moment due to unpaired electrons in partially filled orbitals. See Figure 1.4. As the spin moment is much larger than the orbital moment, the behavior of paramagnetic materials when placed in a magnetic field will be governed by the behavior of the spin magnetic moments. In an ideal paramagnet a moment's neighbors are sufficiently separated from it so that the individual magnetic moments do not interact

with each other. In the presence of a field, the uncompensated spin moments tend to align in the direction of the field and the materials are attracted to the magnetic field, resulting in a net positive magnetization and positive susceptibility. See Figure 1.5.

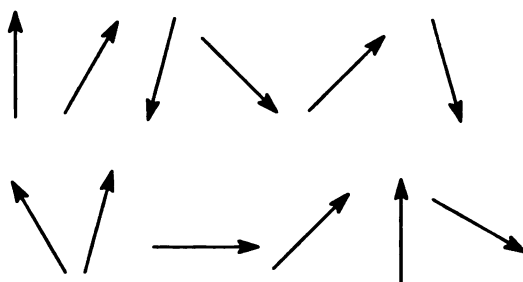
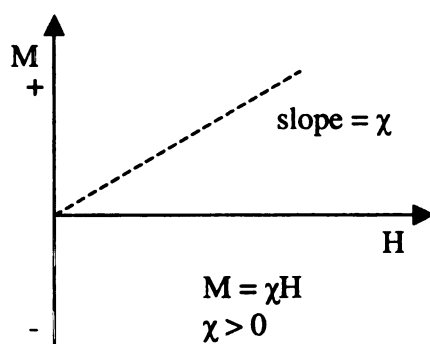
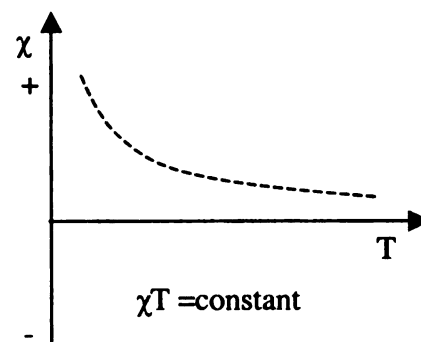


**Figure 1.4.** Paramagnet disordered spins.



(a)



(b)

**Figure 1.5.** Paramagnetism. (a) Magnetization as a function of magnetic field. (b)

Magnetic susceptibility as a function of temperature.

In addition, ideal paramagnetism is characterized by a susceptibility which varies inversely with temperature, see Figure 1.6. Pierre Curie investigated temperature dependence of susceptibility and found that it was equal to  $\chi = C/T$  where  $C = c \mu_0 \text{ Nm}^2/\text{k}$  and is known as the Curie constant.

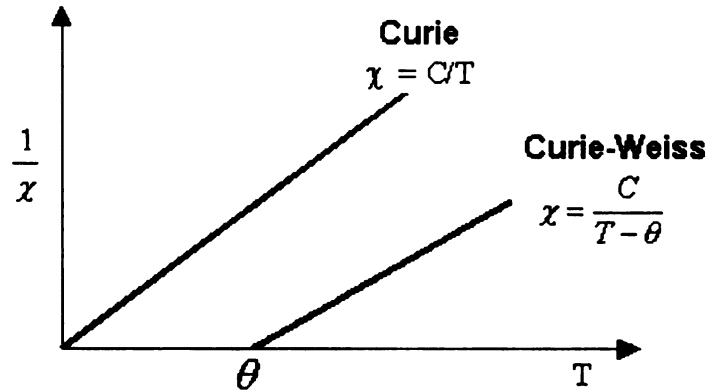


**Figure 1.6.** Paramagnetism showing Curie and Curie-Weiss laws.

Curie's law however is only a special case of the more general Curie-Weiss law  $\chi = C / T - \theta$ . Ideal paramagnetism is the exception rather than the rule because there is normally an appreciable exchange coupling between the ionic moments in a solid. At high temperatures the thermal energy of the moments dominates but as the temperature is lowered it can be seen that a critical temperature occurs at  $T = \theta$  where the susceptibility goes to infinity. An infinite susceptibility means that even in a zero applied field a material can have a finite magnetization. Therefore by reducing the thermal energy of the moments in a paramagnetic material an order-disorder boundary is reached. Below this disordering temperature different magnetic state exists. When it is a ferro- or ferrimagnetic material this temperature is known as the Curie temperature  $T_c$  and for an antiferromagnetic material it is called the Neel temperature  $T_N$ .



### **(III). Ferromagnetism, Ferrimagnetism and Antiferromagnetism**

All three of these classes of materials can be considered a special case of paramagnetic behavior. The description of paramagnetic behavior is based on the assumption that every molecule behaves independently. The materials discussed here result from a situation in which the direction of the magnetic field produced by one molecule is affected by the direction of the magnetic field produced by an adjacent molecule, in other words, their behavior is coupled. If this occurs in a way in which the magnetic fields all tend to align in the same direction, a ferromagnetic material results and the phenomenon is called ferromagnetic coupling. Antiferromagnetic coupling gives an equal number of magnetic fields in opposite directions. Ferrimagnetic coupling gives magnetic fields in two opposite orientations with more in one direction than in the other.

In the presence of an external magnetic field, the tendency of molecules to align themselves to one another enhances the magnetization of the material. This is why ferromagnetic and ferrimagnetic materials can have magnetic susceptibilities several orders of magnitude larger than paramagnetic materials. Also the magnetic susceptibility of these materials is not independent of the magnitude of the external magnetic field as was the case for diamagnetic and paramagnetic materials.

Normally the magnetic moments are aligned in some typical regions (called domain) instead of through out the entire material. Vibrational motion of the molecules, which increases with temperature, can disrupt the domain structure. Thus the magnetic properties of all three of these types of materials are strongest at low temperatures. At sufficiently high temperatures, no domain structure is able to form and therefore all of

these materials become paramagnetic. The temperature at which paramagnetic behavior is seen is called the Curie temperature ( $T_C$ ) for ferromagnetic and ferrimagnetic materials; It is called the Neel temperature ( $T_N$ ) for antiferromagnetic materials.

### **(i). Ferromagnetism**

The elements Fe, Ni, and Co and many of their alloys are typical ferromagnetic materials. Ferromagnetic materials exhibit parallel alignment of moments resulting in large net magnetization even in the absence of a magnetic field - they are "permanently" magnetized (spontaneous magnetization). Ferromagnets can retain a memory of an applied field once it is removed. This behavior is called hysteresis and a plot of the variation of magnetization with magnetic field is called a hysteresis loop. See Figure 1.7 and Figure 1.8.

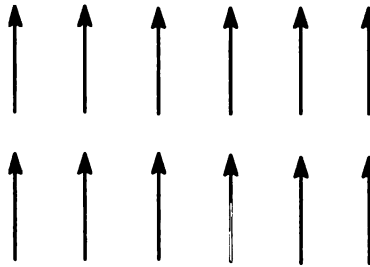


**Figure 1.7.** Parallel alignment of spins in ferromagnetic materials.

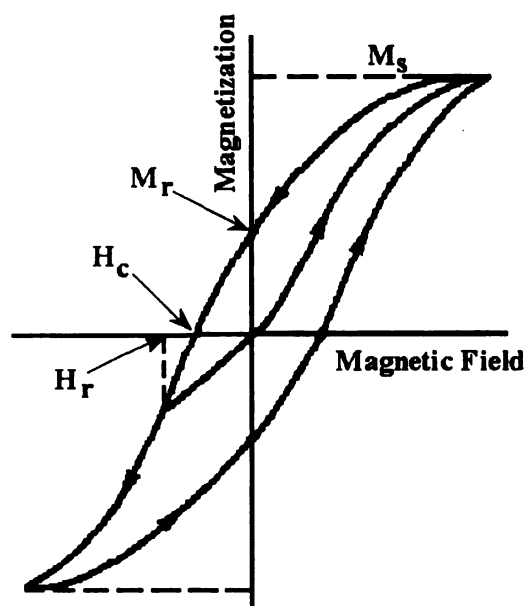


**Figure 1.8.** Typical hysteresis loop for an ordered ferro- or ferrimagnet.  $M_s$ : Saturation magnetization;  $M_r$ : Remanent magnetization;  $H_c$ : Coercive field;  $H_r$ : Coercivity of remanence.

Ferromagnetic compounds show a decrease in magnetic susceptibility with increasing temperature. However, a plot of magnetic susceptibility vs. temperature shows a different line shape from that of paramagnetic compounds. This plot would have a positive curvature for paramagnetic compounds and a negative curvature for ferromagnetic compounds. A rough sketch of the shapes of these curves is shown in Figure 1.9.

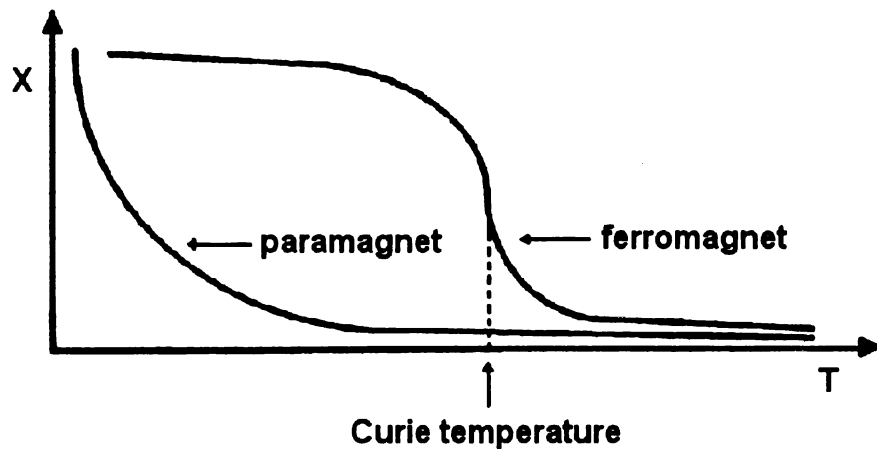


**Figure 1.9.** Magnetic susceptibility vs. temperature curve for ferromagnetic and paramagnetic materials.

## (ii). Ferrimagnetism

Ferrimagnetism is similar to ferromagnetism. It exhibits all the hallmarks of ferromagnetic behavior - spontaneous magnetization, Curie temperature and hysteresis. However, ferro- and ferrimagnets have very different magnetic ordering. Ferrimagnetic compounds such as  $\text{Fe}_3\text{O}_4$  and  $\text{GdCo}_5$  have unpaired electron spins held in a pattern with some up and some down, but there are more spins held in one direction. See Figure 1.10. This gives rise to a relatively strong magnetization.

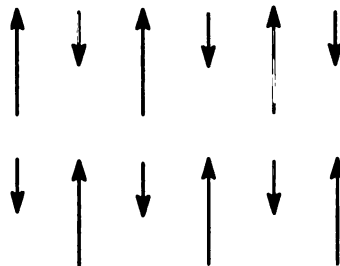


**Figure 1.10.** Antiparallel alignment of spins in ferrimagnetic materials.

The temperature dependence of ferrimagnetism is similar to that of ferromagnetism. In ferrimagnets, however, the spontaneous magnetization,  $M_s$ , usually decreases more rapidly with increasing temperature up to the Curie temperature and in the paramagnetic range there is appreciable curvature from the Curie-Weiss law, particularly close to  $T_c$ .

### (iii). Antiferromagnetism

In antiferromagnetic compounds such as CoO and MnO, the unpaired electrons are held in an alignment with an equal number of spins in each direction, the materials are strongly repelled by a magnet. See Figure 1.11.

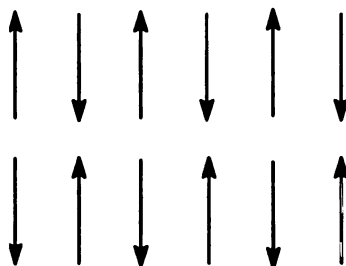


**Figure 1.11.** Antiparallel alignment of spins in antiferromagnetic materials.

There is an order-disorder phase transition from antiferromagnetism to paramagnetism in this type of material at a critical temperature known as the Neel temperature ( $T_N$ ). Antiferromagnetic compounds show an increase in magnetic susceptibility until  $T_N$  is reached. Above  $T_N$ , the susceptibility obeys the Curie-Weiss law

for paramagnets but with a negative intercept indicating negative exchange interactions. See Figure 1.12.

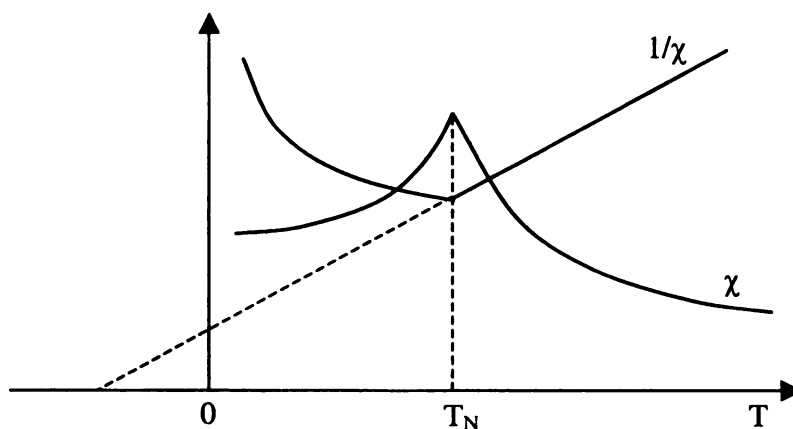


**Figure 1.12.** Magnetic susceptibility vs. temperature curve for antiferromagnetic materials.

### 1.2.2. Molecule-Based Magnets

Molecule-based magnets are a broad, emerging class of magnetic materials. Worldwide interest in molecule-based magnets has risen for both fundamental scientific and technological reasons. Molecule-based magnets are magnetic materials made by means of organic synthetic methodologies, rather than by means of the high-temperature metallurgical methods typically used to make magnets. Essentially all of the common magnetic phenomena associated with conventional transition-metal and rare-earth-based magnets can be found in molecule-based magnets. During the past decade, several classes of molecule-based magnets have been prepared, and new phenomena have been observed. Molecular level magnets expand the materials properties typically associated

with magnets to include low density, transparency, electrical insulation, and low-temperature fabrication, as well as combine magnetic ordering with other properties such as photoresponsiveness.

Conventional magnets rely on metal-atom/ion-based *d* or *f* orbital spins that couple to each other via a structure having direct bonding to other spin sites in three dimensions. However, molecule-based magnets rely on spins residing in *p* orbitals. It is not necessary that the structure of these magnets have covalent bonding to the other spin sites in any dimension. Many molecule-based magnets contain metal ions, however, the organic moieties present in these molecules are key to their magnetic behavior. The organic fragment provides a means to couple as well as contribute spins. The use of spins residing on organic moieties in magnets is in stunning contrast to the behavior of classical magnets.<sup>18</sup>

### **1.2.3. Magnetic conductors**

The search for molecular and polymeric materials combining conductivity with magnetism constitutes a contemporary challenge in materials chemistry research. The efforts in this direction have led to the design of hybrid materials formed by two molecular networks, such as anion-cation salts where each network furnishes distinct physical properties. Examples include organic-inorganic materials combining metal complexes that act as structural or magnetic components with  $\pi$ -electron donor or acceptor molecules that furnish the pathway for electronic conductivity. E. Coronado and coworkers explored the different approaches to construct magnetic conductors and

grouped their recent achievements in three main areas: (1) molecular magnetic conductors based upon tetrathiafulvalene(TTF)-type donors and discrete metal complexes and clusters (metal halides, metal cyanides, metal oxalates, polyoxometalate cluster, etc.), (2) conducting molecular ferromagnets based upon extended magnetic layers incorporating donors in between the inorganic layers and (3) conducting polymers incorporating magnetic complexes and clusters.<sup>19,20</sup>



### 1.3. References

1. (a) Rose JD, Stratham ES. *J. J. Chem. Soc.* **1950**, 69; (b) Hating H. J. *J. Polym. Sci.* **1961**, 51, 526; (c) Manefee E, Pao Y. J. *J. Chem. Phys.* **1962**, 36, 3471.
2. Ito T, Shirakawa H, Ikeda S. *J. polym. Sci.; Polym. Chem.* **1974**, 12, 11.
3. Shirakawa H, Louis EJ, MacDiarmid AG, Chiang CK, Heeger AJ. *J. Chem. Soc.; Chem. Commun.* **1977**, 578.
4. Clarke TC, Geiss RH, Kwak JF, Street GB. *J. Chem. Soc.; Chem. Commun.* **1978**, 489.
5. J.H. Schon, A. Dodabalapur, Z. Bao, C. Kloc, O. Schenker and B. Batlogg. *Nature.* **2001**, 410,189.
6. Seymour RB (ed.). *Conductiive Polymers. Plenum Press. New York.* **1981**, 23-47.
7. Bing R. Hsieh and Yen Wei. *Semiconducting Polymers.* Washington, DC. **1999**, 1-2.
8. Billingham Nc, Calvet PD. Electrically conductive polymers-a polymer science view point. In *Advances in Polymer Science*, vol. 90. Springer-Verlag: Berlin, **1989**, 34-35.
9. (a) A. Andreatta, Y. Cao, J.C. Chiang, A.J. Heeger and P. Smith. *Synth. Met.* **1988**, 26, 383; (b) S. Hotta, S. Rughooputh and A.J. Heeger. *Synth. Met.* **1987**, 22, 79.
10. M. B. Armand, *Adv. Mater.* **1990**, 2, 278.
11. J.R. Reynolds et al., *Macromolecules.* **1992**, 25, 4832.
12. Croce, F., Appetecchi, G. B., Persi, L. and Scrosati, B. *Nature.* **1998**, 394, 456-458.
13. Eduardo Ruiz-Hitzky. *Advanced Materials* **1993**, 5, No. 5, 334-340.
14. Zlatka Gadjourova, Yuri G. Andreev, David P. Tunstall and Peter G. Bruce. *Nature.* **2001**, 412, 520-523.
15. Bruce, P.G. (ed.). *Solid State Electrochemistry* ( Cambridge University Press, Cambridge, **1995** ).
16. Inaguma, Y. et al., *Solid State Commun.* **1993**, 86, 689-693.
17. MacFarlane, D. r., HUANG, j. H. AND Forsyth, M. *Nature.* **1999**, 402, 792-794.

18. Joel S. Miller and Arthur J. Epstein. *MRS Bulletin*. November **2000**, 21-28.
19. Eugenio Coronado, José R. Galán-Mascarós, Carlos Giménez-Saiz and Carlos J. Gómez-García. *Adv. Mater. Opt. Electron.* **1998**, 8, 61-76.
20. M. Clemente-León, E. Coronado, J. R. Galán-Mascarós, C. J. Gómez-García, C. Rovira and V.N. Lauhkin. *Synthetic Metals* **1999**, 103, 2339-2342.

## **Chapter 2. Solvated Electrons, Electrides and Alkalides**

## **2.1. Solvated Electrons**

### **2.1.1. Introduction**

The blue color, paramagnetism and electrical conductivity of solutions of alkali and alkaline earth metals in ammonia, have been known for more than a century.<sup>1</sup> The most satisfactory explanation of the properties of these solutions is in terms of ionization of the metal to its ion and an electron, and subsequent solvation of the ions. The concept of a solvated electron can satisfactorily account for the blue color of these solutions. As the term “solvated electron” implies, the electrons do not exist in solution as free particles, they are solvated, *i.e.*, bound by the solvent. Solvated electrons take part in numerous chemical processes, such as metabolism, photosynthesis, and biological radiation damage.

### **2.1.2. Methods of Producing Solvated Electrons**

Dissolved electrons occur as reaction intermediates in the course of many energy-consuming chemical processes. They are formed on radiolysis, photolysis, and electrolysis of aqueous and other polar systems. They also occur in the base-promoted ionization of hydrogen in solution, and probably in some redox processes.

## (I). Solutions of Metals

Blue colored solutions of electrons in ammonia and amines can be relatively easily prepared by dissolution of alkali metals, alkaline earth metals, and certain rare earth metals, which spontaneously dissociate:  $M \longrightarrow M^+ + e^-$ . In dilute solutions, the electrons are far enough apart to exhibit the spin paramagnetism expected for free spins. The EPR spectrum consisted a single narrow line with electron relaxation dominated by modulation of the hyperfine coupling to nitrogen nuclei. At alkali-metal concentrations greater than  $10^{-3}$  M, dimerization of the species occurs to give entities such as  $e_2^{2-}$ .<sup>2</sup>

In some aliphatic ethers such as tetrahydrofuran, dimethoxyethane, and dioxane, the solubility of alkali metals is three to five orders of magnitude lower than that in ammonia.<sup>3-5</sup> These solutions are also blue, however, they are diamagnetic, probably because of the formation of higher ion pairs or spin-compensated electron pairs. Above 0°C these solutions become colorless.

Solutions of alkali metals in water and alcohols are not stable. However, it is now considered that solvated electrons are produced, but due to the acidic nature of the solvents, they are rapidly transformed into H atoms and eventually hydrogen gas.

The reaction of alkali metals with ice also produces solvated electrons. Bennett et al.<sup>6</sup> deposited alternate layers of ice and alkali metals together at 77°K, in sandwich formation. The resulting product was deep blue and the EPR spectrum consisted a single narrow line. On warming or exposure to visible light, the color and EPR spectrum faded simultaneously.

## **(II). Radiolytic Processes**

Blandamer et al.<sup>7</sup> reported that *F* centers or solvated electrons are produced in the  $\gamma$ -radiolysis of NaOH and KOH glasses at 77°K. Jortner and Sharf<sup>8</sup> also observed the blue color of solvated electrons in the X-irradiation of alkaline glasses at 77°K.

Many radiation-chemical reactions in water, alcohols, and other polar solvents proceed via solvated electrons which are formed after thermalization of high energy electrons produced by Compton effect, the photoelectric effect, and by electron impact.

## **(III). Photochemical Processes**

As far back as 1928,<sup>9</sup> it was proposed that the UV spectra of halide ions in water are due to a transfer of the electron from the halide ion to the solvent. The UV illumination of metals, e.g. mercury, in aqueous solutions leads to the formation of solvated electrons which can be traced by the photocurrent.<sup>10-11</sup>

Solvated electrons take part in many photochemical reactions in aqueous and alcoholic solutions. However, the electrons in photochemical reactions are formed by ionization of photochemically active solutes (e.g.  $\text{Hal}^-$ ,  $\text{OH}^-$ ,  $\text{SO}_4^{2-}$ ,  $\text{CO}_3^{2-}$ ,  $[\text{Fe}(\text{CN})_6]^{3-}$ , and many aromatic compounds having electron-donating groups). This is unlike radiolytic reactions, in which electrons are formed by ionization of the solvent.

#### **(IV). Electrolysis**

It was observed that when solutions of alkali metal salts in ammonia are electrolyzed they attain the blue color of solvated electrons at the cathode.<sup>12</sup>

#### **(V). Dissociation of Hydrogen**

Not only hydrogen atoms, but also hydrogen molecules, can dissociate in the presence of strong bases to give solvated electrons.<sup>13,14</sup>

### **2.1.3. Properties of Solvated Electrons**

#### **(I). Lifetimes of Solvated Electrons**

The high reduction potential of the electrons makes them extremely reactive toward many dissolved ions, free radicals, and neutral molecules, as well as toward the solvent molecules themselves, so that they are generally short-lived and are consequently present in the solutions only in very low concentrations. The lifetimes of the solvated electrons in pure water  $< 1$  msec; The lifetime in pulse radiolysis experiments are usually of the order of  $\mu\text{sec}$ ; Half-lifetimes up to  $10\mu\text{sec}$  may be obtained during the pulse radiolysis of alcohols, although in the flash photolysis of iodide in ethanol, the lifetime is longer ( $\sim 25\mu\text{sec}$ ).<sup>2</sup>

The electrons can be stabilized, however, by inhibition of their reactions in frozen solvents. In the absence of impurities, they have a relatively long life even at room temperature in solutions of metals in ammonia, so that these solutions are particularly suitable for the study of the physical properties of dissolved electrons (rate of decomposition of highly purified sodium-ammonia solutions < 1% per day).<sup>15</sup>

## **(II). Light Absorption**

The most outstanding physical property of solvated electrons is their high light absorption in the red to infrared region of the spectrum, as a result of which they appear blue and can be detected in concentrations as low as  $10^{-8}$  mole/l. The spectrum of dissolved electrons consists of a single broad asymmetric absorption region with a half-width of *ca.* 0.5-1 eV. The area under the absorption curve yields an oscillator strength of nearly unity. The position and height of the absorption maximum depend on the solvent.

The absorption of the solvated electron is interpreted as being due to a  $1s \rightarrow 2p$  transition of a caged electron.<sup>16</sup> The fact that the spectrum extends over a wide range of energies is probably due to a wide scatter of the size of the cavities about a preferred mean value. The asymmetry could arise from unresolved transitions to higher levels, but it has also been attributed to a distribution of cavity sizes.<sup>17</sup>



### **(III). Magnetic Properties**

At very dilute solutions, solvated electrons are paramagnetic (spin paramagnetism). At higher concentrations they tend to undergo spin compensation with formation of diamagnetic electron pairs ( $e_2^{2-}$ ) and the molar susceptibility decreases rapidly. If the concentration of the electrons can be further increased, the solutions assume a metal-like character (free electrons), with high conductivities and metallic luster.<sup>15</sup>

When the solvated electron concentration is very low, the EPR spectrum contains a single, extremely sharp line. The line sharpness and the absence of any hyperfine splitting indicate that there is no strong magnetic interaction between the electron and the solvent molecules of an ordered solvation sheath, but that the solvation sheath forming the cavity must instead be very loosely bound. The spin-compensated electron pairs do not give an EPR signal.<sup>15</sup>

Numerous magnetic measurements have been carried out on solutions of alkali metals in ammonia and other amines. The interpretation of these measurements is complicated because these solutions are complex mixtures of solvated electrons, ion pairs and other loosely bound aggregates, metal-containing diamagnetic species such as  $M_2$  or  $M^+$ , and one or more monomer species,  $M$ .<sup>18</sup>

#### **(IV). Electric Mobility**

Data on the mobility of solvated electrons can be obtained from conductivity studies of their solutions.<sup>19</sup> The mobility of the electron pairs is only slightly lower than that of the unpaired electrons.<sup>15</sup> Thus the marked decrease in the molar magnetic susceptibility on formation of electron pairs has no parallel in the conductivity behavior.

Although the electron is attracted to a rather large polarization center, its mobility exceeds that of ordinary ions in the same solvent. For example, in liquid ammonia the mobility of the solvated electron is about eight times that of a sodium ion,<sup>20</sup> while in water<sup>21</sup> it is less than four times that of a sodium ion. The observed mobility is much smaller than would be expected for a free electron, but it is high enough to require an electron-jump mechanism rather than migration of the entire cavity.<sup>18</sup>

#### **(V). Reactions with Aromatic Compounds**

The reactivity of  $e^-_{aq}$  with aromatic compounds has received detailed study. The aromatic hydrocarbons, owing to their particular electron system, can readily accept an additional electron. This results in the formation of aromatic radical-anions, which are very stable, at least in nonaqueous solutions. They can be prepared in solutions of alkali metals in liquid ammonia, amines, and ethers by the addition of aromatic compounds.

Benzene, is unreactive, whereas substitution in the aromatic ring leads to variation of the reaction rate within wide limits. The effect of substituents in the reactivity of aromatic compounds toward solvated electrons is similar to that shown by the aromatic

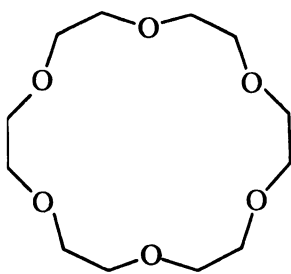
compounds toward nucleophilic reagent. This suggests that dissolved electrons attack the ring system in exactly the same way as nucleophilic reagents, which can be expressed by Hammett's  $\sigma$ -function.<sup>22</sup>

## 2.2. Electrides and Alkalides

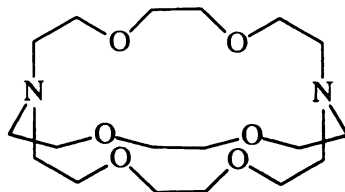
### 2.2.1. Introduction

Electrides ( $M^+L.e^-$ ) and alkalides ( $M^+L.M^-$ ) are ionic salts in which trapped electrons or alkali metal anions ( $Na^-$ ,  $K^-$ ,  $Rb^-$ , or  $Cs^-$ ) serve to balance the charge of complexed alkali cations.<sup>23</sup> Electrides and alkalides have much in common with alkali metal solutions in ammonia, amines, polyethers and other solvents. Solutions of any alkali metal except lithium in amines and ethers contain not only the alkali metal cation,  $M^+$ , and the well-known solvated electron,  $e^-_{solv}$ , but also the alkali metal anion,  $M^-$ . Alkali anions are also known in the gas phase.<sup>24-26</sup>

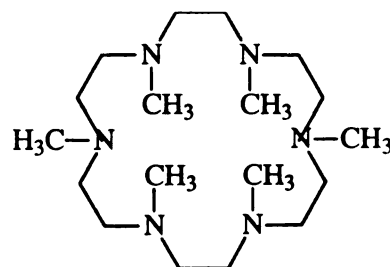
The synthesis of electrides and alkalides was made possible in the late 60's and early 70's when two new types of cation complexing agents, crown ethers and cryptands were synthesized.<sup>27, 28</sup> The addition of strong complexants (L) for the alkali metals provides a new kind of species,  $M^+L_n$  ( $n = 1$  or  $2$ ). Complexation of the cation by crown ethers, cryptands, or methylated aza-crown ethers, not only greatly enhances metal solubility, but also provides enough stabilization of  $M^+$  for alkalide salts.



18-crown-6  
(18C6)



Cryptand [2,2,2]  
(C222)



Hexamethyl Hexacyclen  
(HMHCY)

### 2.2.2. Crystalline Alkalides

Since the first alkalide  $\text{Na}^+(\text{C222})\cdot\text{Na}^-$  was synthesized and characterized in 1974<sup>29</sup>, most of the alkalides prepared so far have been sodides. This is primarily because sodides are generally both kinetically and thermodynamically more stable than potassides, rubidides and caesides. Although salts of alkali metal anions have usually been viewed as exotic, highly unstable compounds, a number of sodides are stable *in vacuo* or under an inert atmosphere for days at room temperatures and indefinitely at freezer temperatures ( $-10^\circ\text{C}$ ).<sup>30</sup>

Although all of the sodides appear distinctly metallic, ranging in color from yellow-gold to dark bronze, they are poor conductors of electricity.<sup>30</sup> Because of the solution equilibrium:  $\text{M}_{\text{solv}}^- \rightleftharpoons \text{M}_{\text{solv}}^+ + 2\text{e}_{\text{solv}}^-$ , it is virtually impossible to synthesize an alkalide that does not contain some trapped electrons and *vice-versa*. Trapped electrons in sodide salts are easily detected by EPR spectroscopy. In general, two types of signals are present: A narrow ( $\sim 0.5$  G linewidth) single line at the free-electron *g*-value

(2.0023) originates from electrons which do not interact preferentially with a single cation or complexant molecule, but rather move rapidly among a number of neighbours to produce a motionally narrow line; A second, broader signal at somewhat lower  $g$ -values, whose position and linewidth depend on temperature, suggest interaction with interstitial or incompletely complexed cations.<sup>30</sup>

### 2.2.3. Electrides Properties

Before the first determination of an electride crystal structure, all earlier work was done with films or powders produced by complete solvent evaporation from solutions which contained  $M^+L$  and  $e^-_{solv}$ . According to the optical and EPR spectra, microwave conductivities and magnetic susceptibilities of electrides, this class of materials showed a variety of electronic properties which further stimulated the search for crystalline electrides. The major breakthrough came when Dheeb Issa, working in Dye group at Michigan State University, discovered the stabilizing influence of dissolved lithium in 2-aminopropane.<sup>31</sup> Once stable solutions could be prepared, crystallization of previously unavailable compounds became possible.

Crystalline electrides are of extreme interest because they are likely to lie at the boundary between metals and non-metals. Electrides fall into three categories: (1) If the electrons are trapped at separate sites that interact only weakly, then one would expect the formation of a paramagnetic insulator or semiconductor. This type of electride was termed as “localized” and represented by  $Cs^+(18C6).e^-$ . (2) If, however, the wavefunctions overlap sufficiently and there are strong interactions between trapped

electrons, a metallic conductor would result. Several electrides, notably  $\text{K}^+(\text{C}_{222})\cdot\text{e}^-$  and  $\text{Li}^+(\text{C}_{211})\cdot\text{e}^-$ , had a plasma-type shape optical spectrum that were similar to those of metallic metal-ammonia solutions. These compounds also had high microwave conductivities, and their magnetic behavior showed substantial inter-electron interactions. This type of electride was “delocalized”. (3) At intermediate levels of interaction, we might expect electron spin coupling to give rise to antiferromagnetic behaviour. Since the electrons would be relatively weakly bound to the cationic lattice, we should observe low-energy photoconductivity and photoelectron emission.

#### **2.2.4. Future Directions**

The wide variety of structures observed for crystalline alkalides and electrides provides examples of isolated metal anions and trapped electrons, cation-anion contact ion-pairs, anion and electron dimmers, and anionic chains. Such variety is made possible by the many choices that are available among complexants and by the ability to select complexants that are appropriate for each of the alkali cations. By using aromatic groups on the complexant, new compounds that contain aromatic radical anions or aromatic dianions that encapsulate an alkali or alkaline earth cation should be possible.

In addition to their appeal in materials research, because of the wide variety of solid-state properties that might be achieved, alkalides and electrides could open new avenues for the study and utilization of alkali metal solutions. By providing relatively stable, concentrated solutions in such aprotic solvents as  $\text{Me}_2\text{O}$  and THF as well as very concentrated solutions in a number of amines, alkalides and electrides open the

possibility of extending metal-ammonia studies to other solvents without the frustrations caused by low solubilities. For the synthetic chemist, the availability of the strongest reducing agents known, as relatively stable solutions in aprotic solvents, should provide new methods for the synthesis of low oxidation state inorganic compounds and organometallic compounds that are difficult to prepare.<sup>32</sup>

### 2.3. References

1. G. Lepoutre and M.J. Sienko, Ed., "*Metal-Ammonia Solutions*". W.A. Benjamin, Inc., New York, N.Y., **1964**.
2. J.K. Thomas. *Radiation Research Reviews* **1968**, 1, 183-208.
3. F.A. Cafasso and B.R. Sundheim. *J. Chem. Physics*. **1959**, 31, 809.
4. J.L. Down, J. Lewis, B. Moore, and G. Wilkinson. *J. Chem. Soc.* **1959**, 3767.
5. F.S. Dainton, D.M. Wiles, and A.N. Wright. *J. Chem. Soc.* **1960**, 4283.
6. J. C. Bennett, B. Mile and A. Thomas. *Nature* **1964**, 201, 919.
7. M. J. Blandamer, L. Shields and M. C. R. Symons. *Nature* **1963**, 199, 902.
8. J. Jortner and B. Sharf. *J. Chem. Phys.* **1962**, 37, 2506.
9. J. Franck and G. Scheibe. *Z. Physik. Chem.* **1928**, 22, A139.
10. G.C. Barker, A.W. Gardner, and D.C. Sammon. *J. Electrochem. Soc.* **1966**, 113, 1182.
11. P. Delahay and V.S. Shrinivasan.. *J. Physic. Chem.* **1966**, 70, 420.
12. H. P. Cady. *J. Physic. Chem.* **1897**, 1, 707.
13. E. J. Kirschke and W.L. Jolly. *Science* **1965**, 147, 45; *Inorg. Chem.* **1967**, 6, 855.
14. U. Schindewolf, R. Vogelsang, and K.W. Boddeker. *Angew. Chem.* **1967**, 79, 1064; *Angew. Chem.* **1967**, 6, 1076.
15. U. Schindewolf. *Angew. Chem.* **1968**, 7, 190.
16. J. Jortner. *J. Chem. Physics*. **1959**, 30, 839; J. Jortner. *Radiat. Res. Suppl.* **1964**, 4, 24.
17. M. J. Blandamer, L. Shields, and M. C. R. Symons. *J. Chem. Soc.* **1965**, 3759.
18. J. L. Dye. *Accounts of Chemical Research* **1968**, 1(10), 306-12.
19. C. A. Kraus. *J. Amer. Chem. Soc.* **1921**, 43, 749; C. A. Kraus and W.W. Lucasse. *J. Amer. Chem. Soc.* **1923**, 45, 2551
20. C. A. Kraus. *J. Amer. Chem. Soc.* **1914**, 36, 864.



21. K. H. Schmidt and W. L. Buck, *Science* **1966**, 151, 70.
22. L. P. Mammett. *Physical Organic Chemistry* **1940**, McGraw-Hill, New York.
23. J. L. Dye, R. H. Huang and D. L. Ward. *J. Coord. Chem.* **1988**, 18, 121-128.
24. S. Matalon, S. Golden and M. Ottolenghi. *J. Phys. Chem.* **1969**, 73, 3098.
25. M. T. Lok, F. J. Tehan and J. L. Dye. *J. Phys. Chem.* **1972**, 76, 2975.
26. J. M. Ceraso and J. L. Dye. *J. Phys. Chem.* **1974**, 61, 1585.
27. C. J. Pedersen. *J. Am. Chem. Soc.* **1967**, 89, 7017; **1970**, 92, 386; *Fed. Proc.* **1968**, 27, 1305; C. J. Pedersen and H. K. Frensdorff. *Angew. Chem., Int. Ed. Engl.* **1972**, 11, 16.
28. B. Dietrich, J. M. Lehn, and J. P. Sauvage. *Tetrahedron Lett.* **1969**, 2885; J. P. Sauvage, J. M. Lehn, and B. Dietrich. *J. Am. Chem. Soc.* **1970**, 92, 2916; J. M. Lehn, *Structure Bonding* **1973**, 16, 1.
29. J. L. Dye, J. M. Ceraso, M. T. Lok, B. L. Barnett, and F. J. Tehan. *J. Am. Chem. Soc.* **1974**, 96, 608.
30. J. L. Dye and A. Ellaboudy. *Chemistry in Britan* March **1984**, 210.
31. D. Issa and J. L. Dye. *J. Am. Chem. Soc.* **1982**, 104, 3781.
32. J. L. Dye. *Journal De Physique IV* **1991**, C5-259-279.

**Chapter 3. Design, Synthesis and Characterization of the Doped  
Poly(glycidyl pentafluorophenyl ether)**

### **3.1. Rationale Design and Structure**

#### **3.1.1. Hexafluorobenzene Radical Anion**

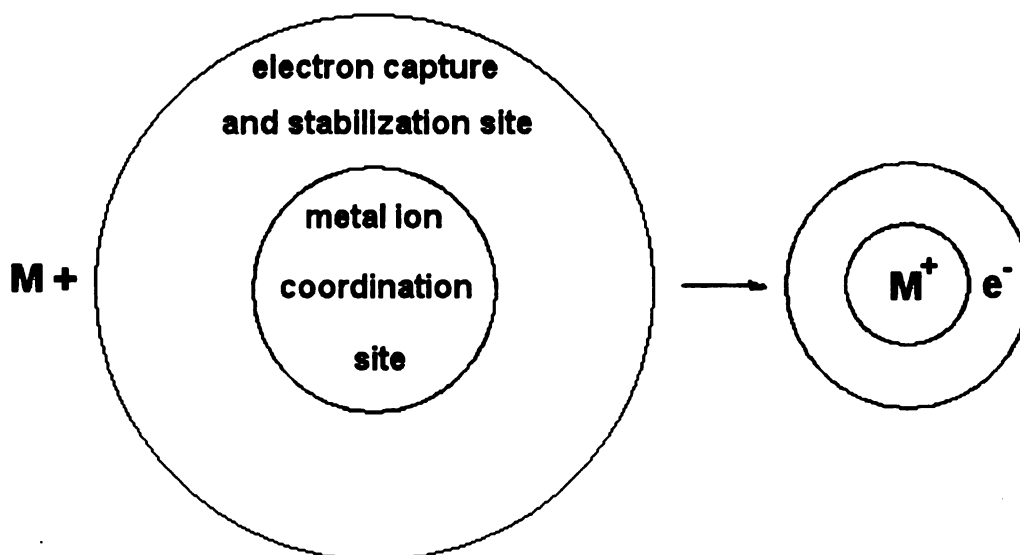
Much theoretical and practical research has been performed on the energetics of electron captured by hexafluorobenzene and on the structure and properties of the resulting radical anion species.<sup>1-9</sup> Hexafluorobenzene has a very high cross section for electron capture. The energy required to bounce the electron back out of the radical anion has been estimated at 0.5 to 0.8eV based on theoretical analyses.<sup>8</sup> Consistent with this, the wavelength of light required to cause the photo-dissociation of the radical anion to a free electron and hexafluorobenzene in the gas phase by laser induced separation has been found experimentally to be ~450nm (2.75eV).<sup>1</sup> This is in the green area of the visible region of the electromagnetic spectrum. In one such study,<sup>8</sup> it was demonstrated that a laser pulse to the radical anion in the gas phase at this wavelength in the presence of an electric potential triggered dissociation and a current pulse that fell to zero within 1 nano second of the end of the laser pulse. The wavelength at which this photodissociation process takes place has special practical significance. If it occurred at lower wavelength (blue or UV) the cost availability of lasers that operate in these areas would be a limitation. If the wavelength were in the red or near IR region then the electron would be so loosely held that the system would be extremely reactive and chemically unstable at room temperature and would reduce most things it came in contact with.

Based on the theoretical and experimental studies performed thus far on the hexafluorobenzene radical anion, solid matrices containing highly fluorinated aromatic

species should have extremely important practical potential. Solid state versions of the laser photolysis experiment described above holds great promise for the development of photo-triggered electronic devices. Condensed phase systems containing high densities of polyfluorinated, aligned aromatic groups are especially interesting because extensive  $\pi$ -orbital overlap involving chains of these aromatic groups will lead to behavior and new bulk properties beyond those possible through simple isolated radical anion formation. Depending on the clustering of energy states and the resulting band formation such systems might behave as semiconductors under some temperature regimes. They may behave as insulators, conductors or superconductors in other temperature domains. Such materials might have useful photochromic or electrochromic properties. For instance, the red color (complementary to the green absorption maximum) in isolated radical anions would be discharged on irradiation and would be quickly re-established on recombination. The application of an electric field that is significantly below the work function of the material in a localized area might alter the energy of the radical anion and hence the color. The combination of electrical and optical effects also opens further avenues. It might even be possible to capture free electrons from sources such as low energy  $\beta$ -emitters. Radioactive sources such as tritium,  $^{14}\text{C}$  or  $^{35}\text{S}$  should be suitable. The ability to capture free electrons is a desirable feature of materials used as high voltage insulators especially in thin film applications. Metals are known for their tendency to donate electrons. An interesting possibility is the fabrication of a system that contains complexation sites for the metal cation so formed thus reducing the overall energetic cost of the formation of delocalized electron species.

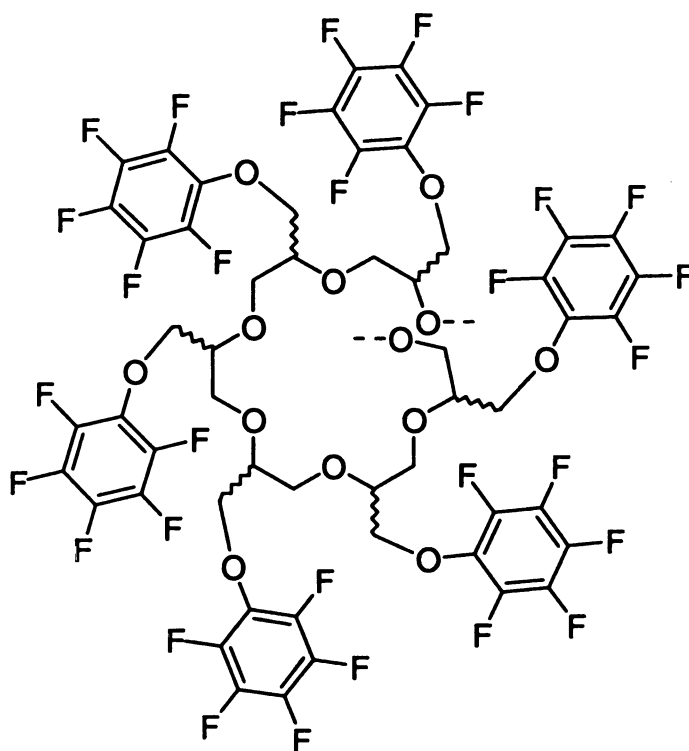
### 3.1.2. Structure of the Doped Poly(glycidyl pentafluorophenyl ether)

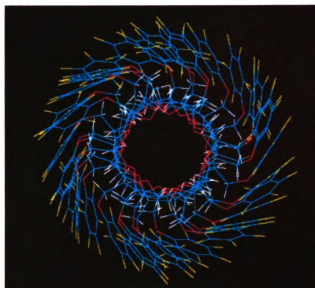
The preparation of a matrix containing high densities of polyfluorinated aromatic groups and very high binding capacity for metal cations was our goal. We decided to use a polyether as the central element with the fluorinated aromatic groups attached as side chains. We envisioned the formation of charge-separated species by the dissolution or dispersion of alkali metals in the matrix. Our expectations were that the alkali cation would complex with the oxygen functions of the polyether and the electron would be captured by the fluorinated groups and exist within some band structure or as a more localized radical anion. Such a system would be much more stable than alkalides (systems in which the electron is captured by a neutral metal atom to form a metal anion) because the electron affinity of hexafluorobenzene (0.5-0.8eV) is much greater than that of an alkali metal atom (~0.3eV).



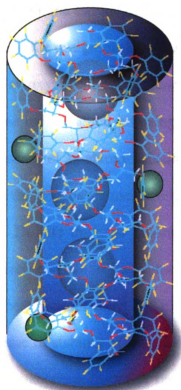
We synthesized a polymer of the general structure shown below. The synthetic strategy is shown in Scheme 3.1. The rationale behind the architecture is quite simple: The poly-ethylene oxide backbone should form a helical structure with the oxygen atoms facing inwards to bind to the metal ions very much as in a crown ether; The pendant pentafluorophenoxymethyl groups should then form an outer whorl around the polyether core (Figure 3.1-a). The major form of this arrangement would be a central cylindrical channel along which the metal ions move surrounded by an outer sheath containing pentafluorophenyl groups and interacting electrons (Figure 3.1-b).

Poly(glycidyl pentafluorophenyl ether):





(a)



(b)

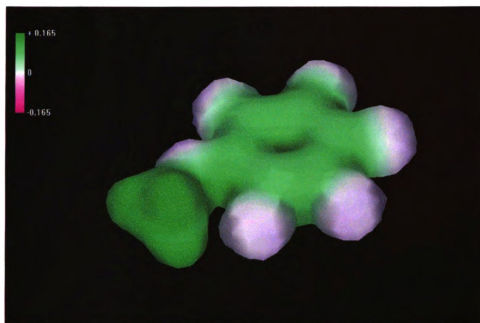
**Figure 3.1.** The structure of poly(glycidyl pentafluorophenyl ether).

The situation described above is an ideal one. Poly(ethylene oxide) really does not exist in a helical conformation to a major extent except in the crystalline state.<sup>10</sup> In the presence of alkali metal cations however, the percentage of gauche conformers about the C-C bond for the dialkoxyethane units (characteristic of the helical structure) increases significantly.<sup>11</sup> This interaction is the essential driving force that promotes metal ion templated crown ether formation. A crown ether molecule complexed with a metal ion will have all gauche conformations about the C-C bonds. In the present situation, regions of transient helicity initiated and stabilized by the alkali metal cation along a significantly less ordered backbone would be formed.

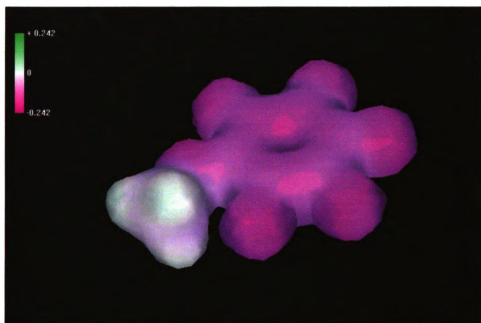
The published information on the stability of the hexafluorobenzene radical anion was an important starting point in the design of the system. One of the first questions to be addressed was whether an alkoxy pentafluorobenzene radical anion had comparable stability to a hexafluorobenzene radical anion allowing us to capitalize on the known properties of the latter. The presence of an alkoxy substituent on the benzene ring should increase the electron density in the ring by the mesomeric effect thus making the capture of the electron less favorable. Despite this, the presence of five fluorine substituents should still have a profound effect in stabilizing a captured electron. Estimates of heat of formation of radical anions of hexafluorobenzene and methoxy pentafluorobenzene using AM1 calculations gave a decrease in stability of only 24% on replacement of a fluorine atom by a methoxy group. The indication from this result was that there would still be tremendous stabilization of the captured electron by the remaining five fluorine atoms. The molecular electrostatic potential surface of the radical anion and the neutral form of



methoxypentafluorobenzene (Figure 3.2) demonstrate the ability of the fluorine atoms to spread the charge over the ring.



(a)



(b)

**Figure 3.2.** Molecular electrostatic potential surface for (a) methylpentafluorophenyl ether and (b) methylpentafluorophenyl ether radical anion calculated using PM3 semi-empirical method.

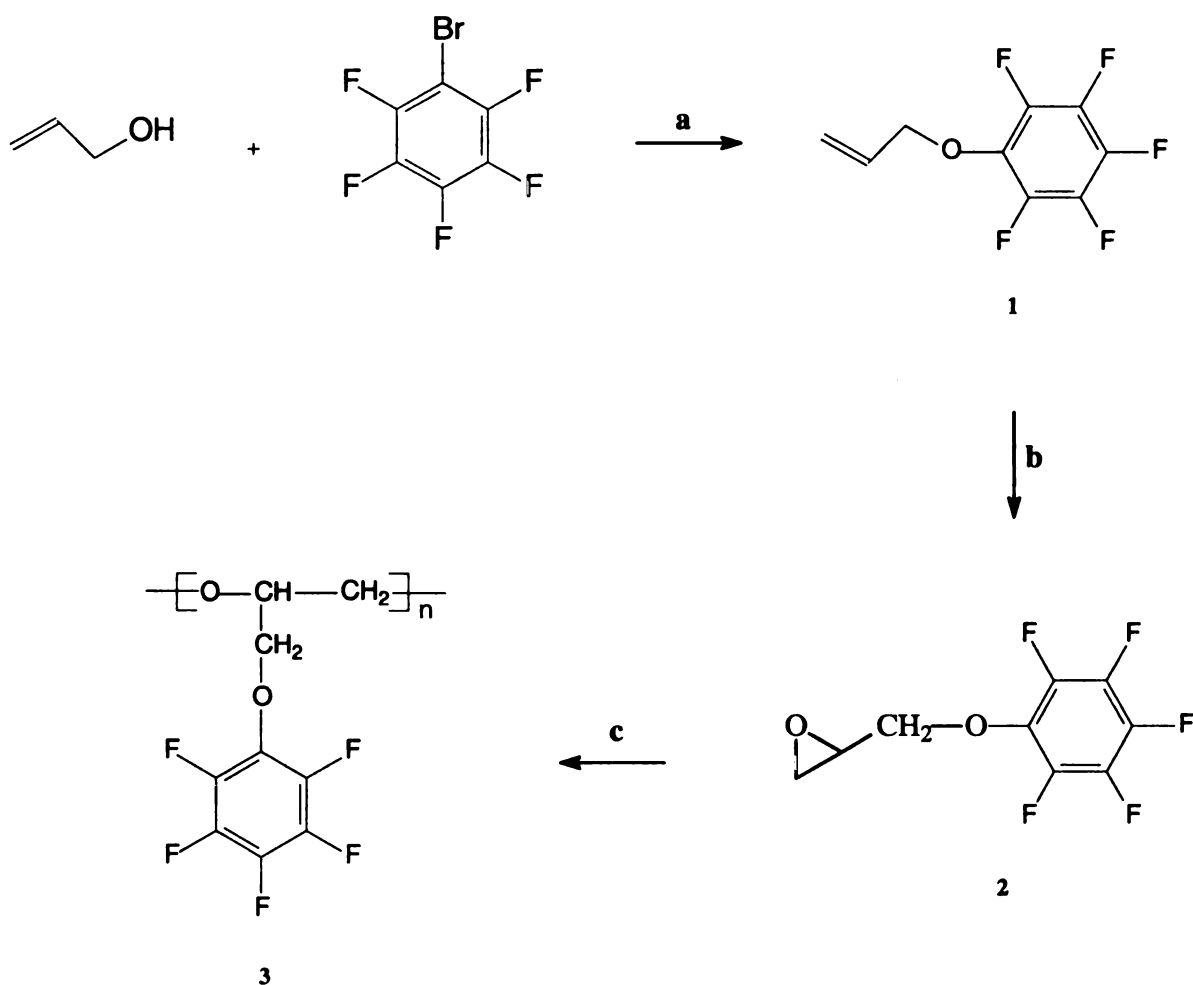
## 3.2. Experimental

### 3.2.1. Synthesis of Poly(glycidyl pentafluorophenyl ether)

All chemicals were used as received from Aldrich unless otherwise noted.

The route to poly(glycidyl pentafluorophenyl ether) is outlined in Scheme 3.1.

**Scheme 3.1** Synthesis of poly(glycidyl pentafluorophenyl ether)



Reagents and conditions: (a) NaH, THF, 25°C, 6h, 100% (crude); (b) mCPBA,  $\text{CH}_2\text{Cl}_2$ , 25°C, 12h, 85% (crude); (c)  $\text{SbCl}_5$ ,  $\text{CH}_2\text{Cl}_2$ , 25°C.

#### **(a). Preparation of allyl pentafluorophenyl ether**

The synthesis began with commercially available allyl alcohol and bromopentafluorobenzene in a  $S_N2$  reaction to give compound 1. The mole ratio of the starting materials was: allyl alcohol/bromopentafluorobenzene/sodium hydride = 5.0/1.0/1.2. Firstly, sodium hydride (60% dispersion in mineral oil) was washed by 50 ml hexanes. After pouring out the hexanes, the reaction solvent THF was added to the flask equipped with a drying tube. The stirrer was started and the temperature was kept at 25°C. Allyl alcohol was added to the sodium hydride solution very slowly to avoid excessive foaming and heat production. Bromopentafluorobenzene was then added drop by drop. The reaction was checked by TLC. After the reaction was done, THF and excess allyl alcohol were removed and  $CH_2Cl_2/H_2O$  was added to the reaction mixture. The organic layer was washed with water thoroughly to remove sodium bromide, it was then dried with anhydrous sodium sulfate and stripped of solvent. The yield of the crude product was almost 100%. The crude product was purified by flash column chromatography using hexanes as the eluant.

#### **(b). Preparation of glycidyl pentafluorophenyl ether**

The epoxidation of compound 1 was performed by treatment with 70 ml of 20% solution of m-chloroperbenzoic acid (mCPBA) in methylene chloride. The temperature was kept at 25°C by cooling during addition of the mCPBA solution over a 10 min period. After the reaction was done, 200 ml 10% sodium sulfite was added to destroy

excess peracid until a test with starch-iodide paper was negative. The reaction mixture was then transferred to a separatory funnel and the organic layer was washed with 200 ml 5% sodium bicarbonate solution to extract the m-chlorobenzoic acid, followed by washing with water and finally with saturated sodium chloride solution. The organic layer was then dried and stripped of  $\text{CH}_2\text{Cl}_2$ . The crude product was purified by column chromatography on silica with 1:1  $\text{CH}_2\text{Cl}_2$ /hexanes. The product was then purified by vacuum distillation. The pure product glycidyl pentafluorophenyl ether is a viscous pale yellow liquid.

**(c). Preparation of poly(glycidyl pentafluorophenyl ether)**

Poly(glycidyl pentafluorophenyl ether) **3** was obtained by cationic polymerization of the corresponding epoxy monomer **2**. Antimony (V) chloride ( $\text{SbCl}_5$ ) was used as the polymerization catalyst. The initial concentrations of the epoxy monomer and catalyst in dichloromethane were:  $[\text{monomer}] = 2.0 \text{ mol/l}$ ;  $[\text{SbCl}_5] = 0.02 \text{ mol/l}$ . The reaction was carried out at  $25^\circ\text{C}$  under argon protection. Polymer **3** was dried under vacuum at ambient temperature. Molecular weight (MW) of polymer **3** was estimated by gel permeation chromatography (GPC) using “Shodex Asahipak GS-310 7G” column and THF as eluant.

### **3.2.2. Doping**

The doped polymeric materials were prepared by reacting alkali metals with the synthesized polymer. The polymer was first fractionated by gel permeation chromatography into high, medium and low molecular weight fractions. The high and medium molecular weight fractions were used.

This step was performed in an argon chamber. Certain amount of polymer was dissolved in THF and metal (potassium, sodium or lithium) was added at room temperature. The temperature was then raised gradually until it was 5°C above the metal's melting point. Keeping the temperature at this value until all of the metal was melted and reacted with the polymer.

### **3.2.3. Characterization of the Materials**

#### **3.2.3.1. Gel Permeation Chromatography**

Gel Permeation Chromatography (GPC) was carried out using a Waters system equipped with a Waters 2414 refractive index detector and a Waters 2487 dual  $\lambda$  absorbance UV detector, with THF as the eluant, at room temperature.

#### **3.2.3.2. FT-IR Spectroscopy**

The FT-IR spectra were recorded on a Nicolet 710 FT-IR spectrometer.

### **3.2.3.3. NMR Spectroscopy**

NMR measurements were made in  $\text{CDCl}_3$  at room temperature on a Varian VXR 500MHz spectrometer.

### **3.2.3.4. UV-visible Spectroscopy**

UV-vis spectra were taken in a Hewlett Packard 8452A diode array spectrophotometer.

### **3.2.3.5. SQUID Measurements**

Magnetic properties of the materials were measured using a Quantum Design MPMS XL SQUID (Superconducting Quantum Interference Device) magnetometer. Samples were transferred to polycarbonate capsules under an atmosphere of dry argon and were loaded at room temperature in zero magnetic field. Both the temperature dependence of mass susceptibility at specific fields and the field dependence of magnetization at specific temperatures were measured. The magnetic moments of the empty capsules were acquired and subtracted from the data.

### **3.2.3.6. Conductivity Measurements**

Electrical resistance measurements were made using the two-probe technique. The doped polymers were dissolved in THF to get a series of solutions with different concentrations. Two platinum electrodes (The diameter of the platinum wire is 0.5mm; The distance between two electrodes is 3mm) were immersed in these solutions and the other ends of the electrodes were connected to a RadioShack auto-ranging digital multimeter to measure the resistance of these solutions. To avoid any contamination these measurements were performed in a glove-box filled with argon. Data were collected at room temperature.

### **3.2.3.7. EPR spectroscopy**

EPR measurements were made on a Bruker ESP 300E spectrometer in high-purity He gas. The doped samples were dissolved in THF and sealed in quartz tubes under argon protection to avoid any contamination.

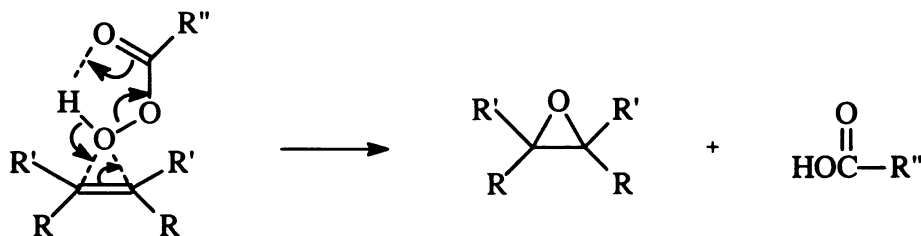


### 3.3. Results and Discussion

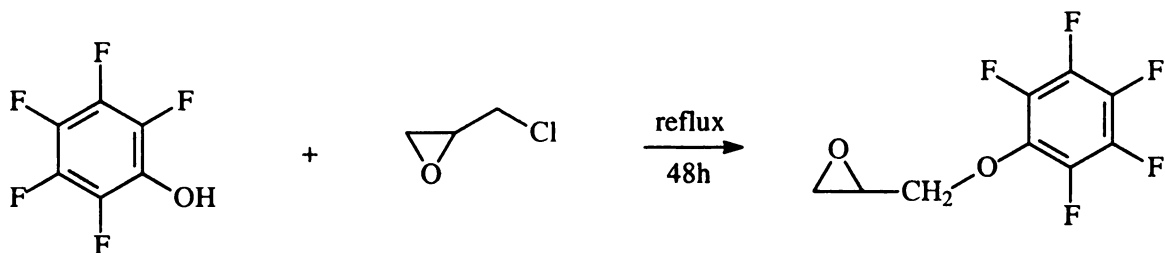
#### 3.3.1. Synthesis of Poly(glycidyl pentafluorophenyl ether)

##### 3.3.1.1. Preparation of Glycidyl Pentafluorophenyl Ether

Glycidyl pentafluorophenyl ether is useful as thinners, especially for epoxy resins. It has been prepared by the epoxidation of the corresponding olefin. The epoxidation of olefins is one of the most important synthetic manipulations due to the broad range of chemistry available to further derivatize epoxides. The most general reagents for conversion of simple alkenes to epoxides are peroxycarboxylic acids. *m*-Chloroperbenzoic acid (mCPBA) is a particularly convenient reagent, it has an electrophilic oxygen that reacts with the  $\pi$  system of the alkene. Addition of oxygen occurs preferentially from the less hindered side of the molecule. It has been demonstrated that ionic intermediates are not involved in the epoxidation reaction. The oxidation is believed to be a concerted process. A representation of the transition state is shown below.



Glycidyl pentafluorophenyl ether can also be prepared by the condensation of pentafluorophenol and epichlorohydrin.<sup>12</sup> These two compounds were refluxed at 80°C in the presence of acetone and H<sub>2</sub>O and further refluxed with addition of NaOH to give 84.6% glycidyl pentafluorophenyl ether.



The <sup>1</sup>H-NMR, <sup>13</sup>C-NMR and <sup>19</sup>F-NMR (hexafluorobenzene was used as external standard) spectra of the synthesized glycidyl pentafluorophenyl ether were shown in Appendix 1, 2, and 3.

### 3.3.1.2. Polymerization of Glycidyl Pentafluorophenyl Ether

Epoxides, like cyclopropanes, are strained due to the constraints imposed by bonding three tetrahedral atoms into a three-membered ring. As a consequence of this ring strain, epoxides undergo ring-opening reactions with nucleophiles via S<sub>N</sub>1 and S<sub>N</sub>2 mechanisms.

The polymer of glycidyl pentafluorophenyl ether was prepared in the presence of a catalyst by cationic or anionic mechanism.<sup>13-18</sup> The polymerization was investigated in several different conditions, as shown in Table 3.1. Poly(glycidyl pentafluorophenyl ether) with the highest molecular weight was obtained in dichloromethane at r.t. by using

SbCl<sub>5</sub> as the catalyst. For cationic polymerization of epoxides, the following Lewis acids can be used as catalysts: stannic chloride (SnCl<sub>4</sub>), stannic bromide (SnBr<sub>4</sub>), stannic iodide (SnI<sub>4</sub>) and antimony (V) chloride (SbCl<sub>5</sub>). According to literature, the highest catalytic activity was shown by SbCl<sub>5</sub> but that of SnCl<sub>4</sub> was only slightly lower. The higher catalytic activity of SbCl<sub>5</sub> relative to that of SnCl<sub>4</sub> may be explained by the higher electrophilicity of the antimonium ion.

Like the polymerization of many epoxy monomers with Lewis acids, instantaneous initiation and rapid decrease of polymerization rate is characteristic of this system. Conversion of glycidyl pentafluorophenyl ether was estimated by <sup>1</sup>H-NMR spectrum of the crude polymerization mixture. Very high initial rate and prompt quenching of polymerization was observed. The MW of the polymer obtained was investigated by GPC. It was found that the MW increased as the initial catalyst concentration increased, but when the concentration of SbCl<sub>5</sub> exceeds 0.02 mol/l, no apparent MW increase was observed.

**Table 3.1.** Polymerization of glycidyl pentafluorophenyl ether with antimony (V) chloride or potassium t-butoxide.

catalyst	solvent	temp (°C)	MW <sup>a</sup>
0.02 mol/l SbCl <sub>5</sub>	CH <sub>2</sub> Cl <sub>2</sub>	25	10000-50000
0.02 mol/l SbCl <sub>5</sub>	CH <sub>2</sub> ClCH <sub>2</sub> Cl	60	< 2000
1% (CH <sub>3</sub> ) <sub>3</sub> COK	DMSO	110	< 2000

<sup>a</sup> Estimated by GPC based on polystyrene standards.

### **3.3.2. Characterization of Poly(glycidyl pentafluorophenyl ether)**

#### **3.3.2.1. Solubility**

Poly(glycidyl pentafluorophenyl ether) exhibits good solubility in common organic solvents such as acetone, chloroform, dichloromethane, THF, DMF and DMSO at room temperature. The excellent solubility is an indication that this processable polymer has enough scope for technological application.

#### **3.3.2.2. GPC Results**

The molecular weight of poly(glycidyl pentafluorophenyl ether) was measured by means of GPC using THF as eluant against polystyrene standards. The average molecular weight and the molecular weight distribution were calculated by means of standard curves shown in Figure 3.4:  $K_{av} = (t_e - t_0)/(t_i - t_0)$  ;  $t_0 = 7.049\text{min}$  based on blue dextran;  $t_i = 12.058\text{min}$  based on glucose;  $t_e$  is the retention time of the measured polymer.

The GPC chromatogram of poly(glycidyl pentafluorophenyl ether) is shown in Figure 3.3-(b). The average molecular weight is 36633. The molecular weight distribution is 10000-50000. This high molecular weight was also confirmed by mass spectrum (MALDI).

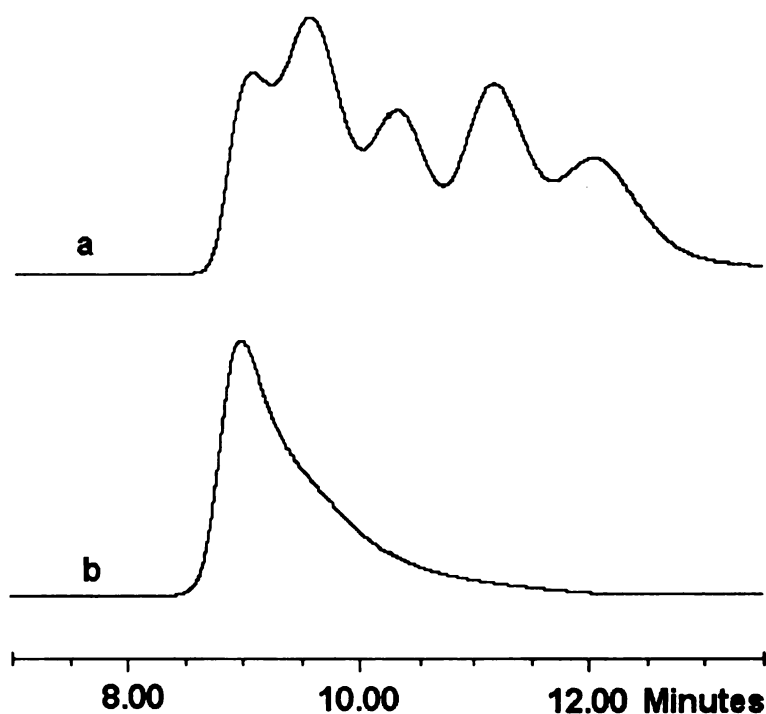


**Figure 3.3.** GPC chromatogram of (a) Polystyrene standards: MW = 38100, 21000, 10050, 4920, 2350; Retention time (min) = 8.675, 9.216, 9.950, 10.783, 11.665. (b) Poly(glycidyl pentafluorophenyl ether): Retention time = 8.640 min.

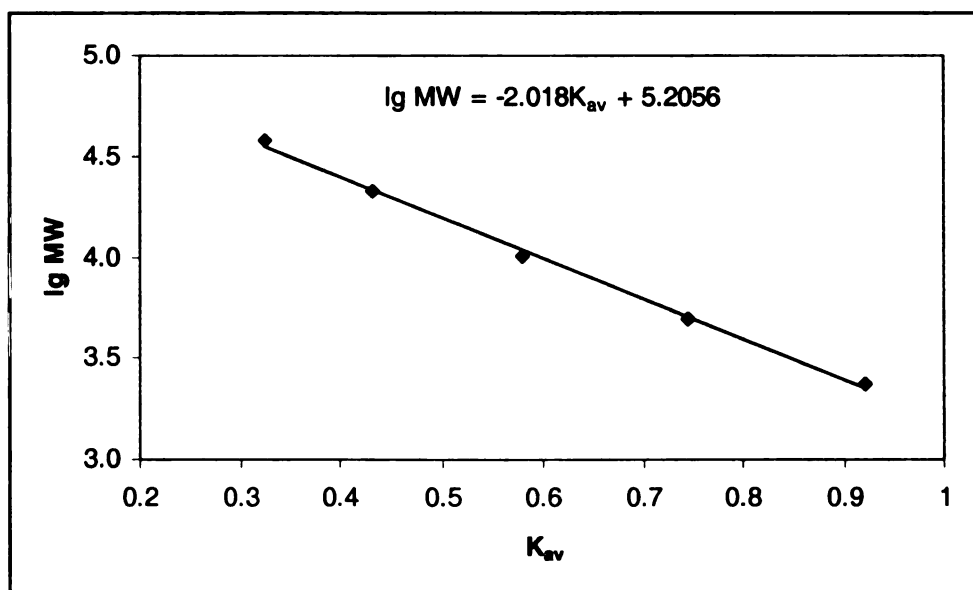


**Figure 3.4.**  $\lg MW$  v.s.  $K_{av}$  standard curve for poly(glycidyl pentafluorophenyl ether).

### **3.3.3. Characterization of the Doped Poly(glycidyl pentafluorophenyl ether)**

Treatment of poly(glycidyl pentafluorophenyl ether) with sodium, potassium or a mixture of these metals in tetrahydrofuran under an argon atmosphere at room temperature led to the rapid but smooth dissolution of the metal and an immediate color change. The pink colors of the solutions were stable for several weeks at room temperature with a minimum of protection from moisture and oxygen. They did vary with the type and, to a great extent, amount of the alkali metal that was used in the doping process.

#### **3.3.3.1. UV-visible Spectra**

The UV-vis absorption spectra of the alkali metal-doped poly(glycidyl pentafluorophenyl ether) were shown in Figure 3.6. Dissolving the doped polymers in THF produced a series of pink color solutions (shown in Figure 3.5) which showed bands in the UV and visible regions. The bands generally showed fine structure (several branches) indicating vibrational coupling to the electronic levels. The absorption bands in the near UV to visible region of the spectrum of the medium molecular weight material doped with 35% sodium appeared between 360 and 460 nm with maxima at 371, 396, 422 and 447 nm. The same material doped with 25% potassium had maxima at 352, 402 and 453 nm. The region in which these bands occurred compared favorably with reported values of 450 nm and 480 nm for the hexafluorobenzene radical anion. Bands in the visible region of the spectrum for the higher molecular weight material generally

appeared at considerably longer wavelengths. Material doped with 20% potassium had bands at 553, 577 and 594 nm however material doped with similar amounts of sodium had bands at 352, 402 and 453 nm. Doping with much higher concentrations of sodium (30%) resulted in bands at 550, 574 590 nm, considerably longer wavelength than was observed with the lower molecular weight material when it was treated with even higher (35%) amounts of sodium.

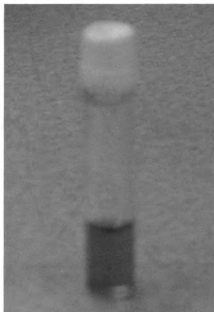


**Figure 3.5.** Solution of the alkali metal-doped poly(glycidyl pentafluorophenyl ether) in THF.

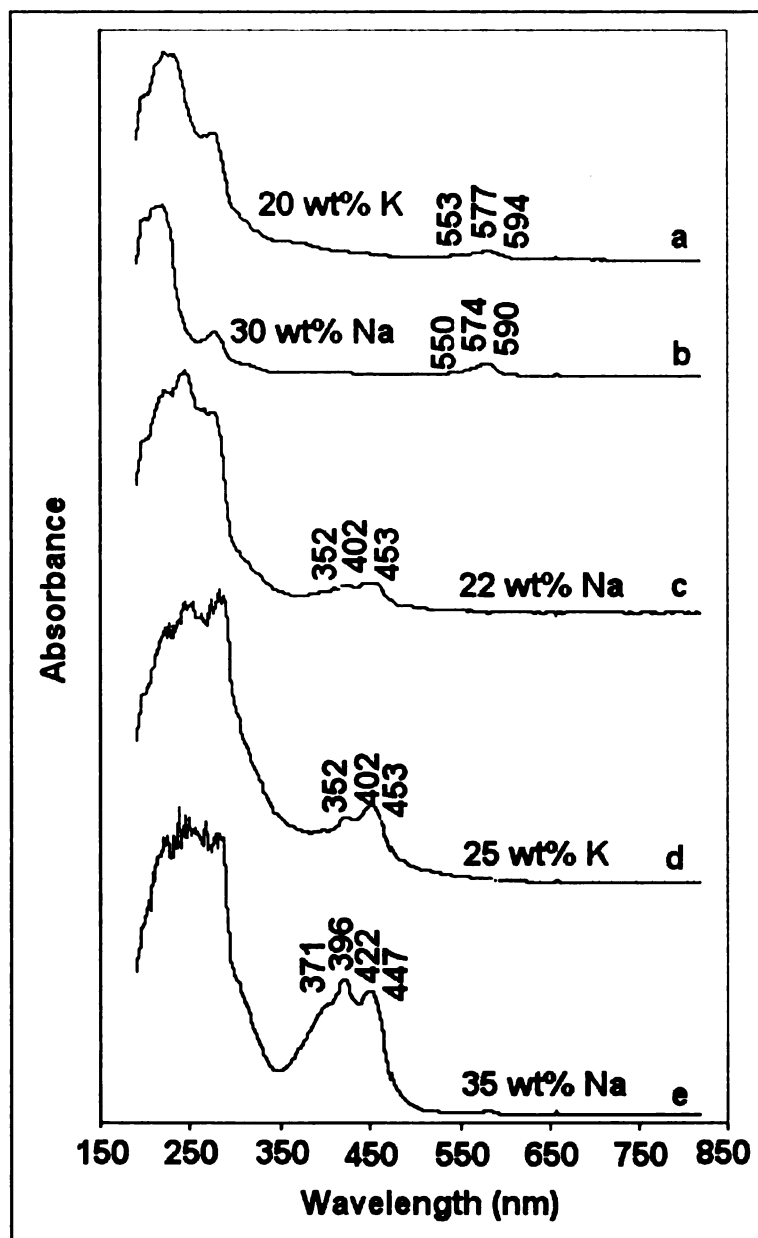
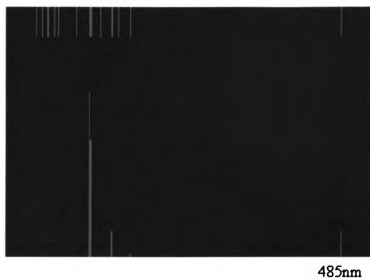


**Figure 3.6.** UV-vis absorption spectra of the doped poly(glycidyl pentafluorophenyl ether). (a) (b) (c): High MW fraction (10000-50000 daltons); (d) (e): Medium MW fraction (2000-10000 daltons).



Zindo calculations of UV-visible spectral frequencies and oscillator strengths for hexafluorobenzene and the model system methoxy-2,3,4,5,6-pentafluorobenzene gave a value of 485 and 519 nm respectively (Figure 3.7). The value of 485 nm is in agreement with experimental results for hexafluorobenzene. The value of 519 nm is between the range observed for the doped medium and high molecular weight polymer.



(a)



(b)

**Figure 3.7.** UV-vis spectra of (a) hexafluorobenzene radical anion and (b) methoxypentafluorobenzene radical anion from Zindo calculations.

The absorption maximum for the high molecular weight material generally occurred at significantly longer wavelength. This 150 nm red shift indicates that there are some stacking interactions that are contributing to a delocalized orbital system or band structure involving several aromatic groups. This will be favored in the higher molecular weight systems because of greater rigidity, a higher density of packing of groups and more regions of crystallinity and order.

The nature and concentration of the metal in the polymeric matrix are two other very important factors in promoting stacking or multicenter interactions that lead to this 150 nm red shift in the visible region of the spectrum. All three of these factors should promote the helical polyether conformation forcing the formation of the pentafluorophenyl sheath around the metallated polyether core thus enabling band formation. Evidence for stacking was raised in a previous study when a concentration-dependent shift in the absorption maximum was noted for hexafluorobenzene.<sup>19</sup> The phenomenon here is more than this. There is not a gradual shift in absorbance but a rather dramatic shift of 150 nm indicating a conformational shift, phase change or change in electronic state. The other dimension of these new materials that is yet to be considered is the nature of the metal species formed on dissociative solvation of sodium and potassium. Several states are possible involving various equilibria between these states. Contributions to these equilibria from metal cations, alkalides, electrides and diatomic metal molecules might all be possible. Such equilibria will affect the electronic state of the aromatic system and have a significant effect on the visible spectra.

### 3.3.3.2. Magnetic Properties

The fate and behavior of the electrons produced by the dissociation of the alkali metal is an important determinant of the properties of the new polyether material. If the electrons are held too tightly in the radical anion they might not be available as charge carriers and the material might be largely paramagnetic. There might be a population of free electrons that could couple strongly giving the material an antiferromagnetic character.  $\pi$ -Orbital overlap between closely spaced and aligned pentafluorophenyl groups should lead to energy bands resulting in new optical, electronic and magnetic properties. Electrons might then readily diffuse through the pentafluorophenyl clusters from ring to ring with varying degrees of coupling with each other. The physical path they take and the nature of the surface is also a question. They could travel around the cylinder in circular or helical paths or they could migrate in a linear fashion from end to end. The path would be very dependent on the presence and strength of magnetic fields.

Magnetic measurements were taken in four different magnetic fields (1000Oe, 3000Oe, 5000Oe and 10000Oe) and the temperature range was 5K-300K. Also measurements were taken in two different temperatures (5K and 300K) and the magnetic field range was 0Oe-10000Oe.

Figure 3.8-(c) shows the temperature dependence of the mass susceptibility ( $\chi_g$ ) of high MW(10000-50000) poly(glycidyl pentafluorophenyl ether) doped with 20 weight % potassium. The classical increase in susceptibility with temperature through a maximum (the Neel point) at constant field and an exponential decay to a limiting value characteristic of antiferromagnetic substances was invariably evident. However,

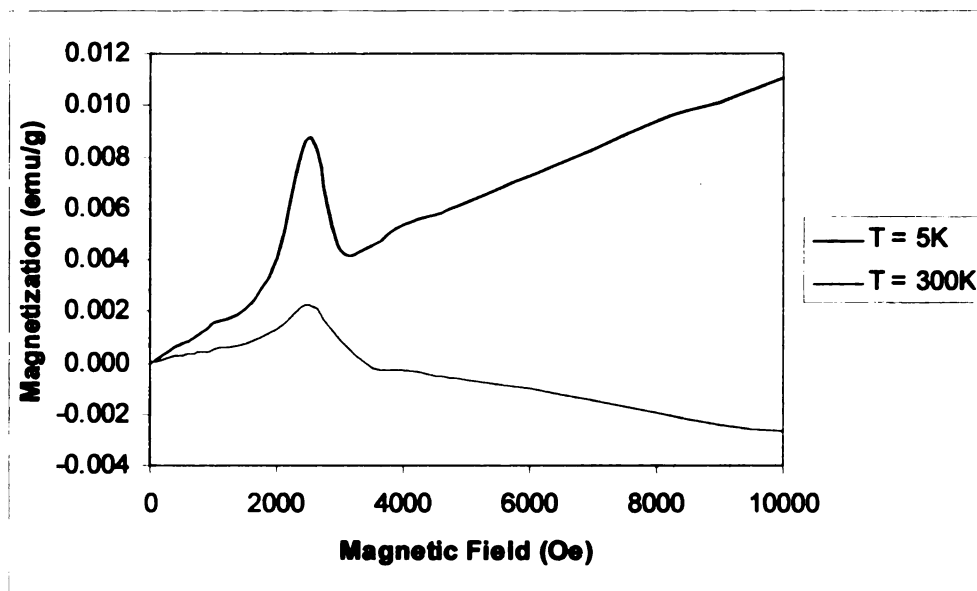
variations on the decay curve past the Neel temperature and variations before the very sharp increase leading up to the Neel temperature were observed. The Neel temperature ( $T_N$ ) is affected by the magnitude of the measuring field, the higher the applied field, the lower the Neel temperature:  $T_N$  is about 40K at 1000Oe, 20K at 5000Oe and 15K at 10000Oe. The field dependence of  $T_N$  is quite consistent with a situation in which the coercive force of a field and the randomizing effects of temperature are acting together to uncouple spins in an antiferromagnetic system. At low fields one would expect the temperature required to be significantly higher.

Figure 3.8-(c) shows a rapid decrease in susceptibility between 5 and 10K before an abrupt increase to the Neel temperature (maximum) for all but the lowest field of 1000 Oe. In this case the susceptibility stayed constant but positive after the initial drop until approximately 30 K before increasing towards the maximum. This complex behavior might indicate some spontaneous (ferrimagnetic) character that is not readily randomized by temperature especially at lower field. The initial drop in susceptibility with increasing temperature in the low temperature regime indicates paramagnetic character. This unusual behavior before the Neel transition is also characteristic of some low-dimensional systems such as 1-dimensional magnetic systems. The sudden drop in susceptibility at low temperature is attributed to defects in the chain. The variation transitions observed at higher temperature (100 to 300 K) attributable to and indicative of the fundamental nature of the new materials. Unlike metals, inorganics and crystals these are essentially soft organic materials that should form organized structures (liquid crystalline phases) at different temperatures and go through various melting and other phase transitions as the temperature is varied. The applied field should be a large factor in

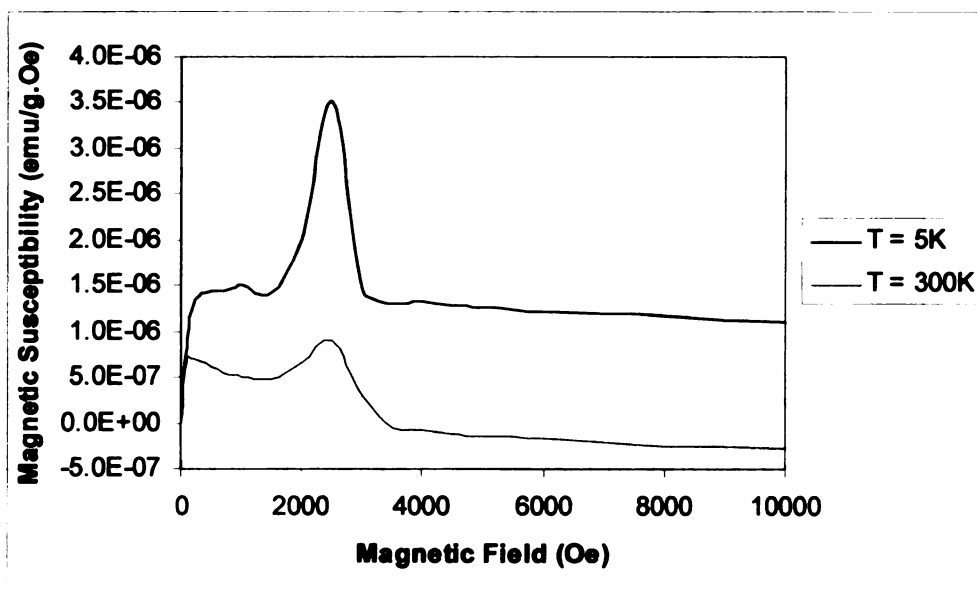
determining the magnetic properties, orientation and stability of these new structures and phases since they will interact with this field. There will be phases that are essentially field induced oriented and stabilized especially at high field. Structures and phases that are stable at lower temperatures can be destroyed as the temperature increases giving rise to the undulations (transitions) observed between 100 and 300 K especially at the higher field values.

Figure 3.8-(a) shows the magnetization vs. magnetic field curves at two different temperatures, non-linearity is clearly observed, confirming the presence of antiferromagnetic interactions.

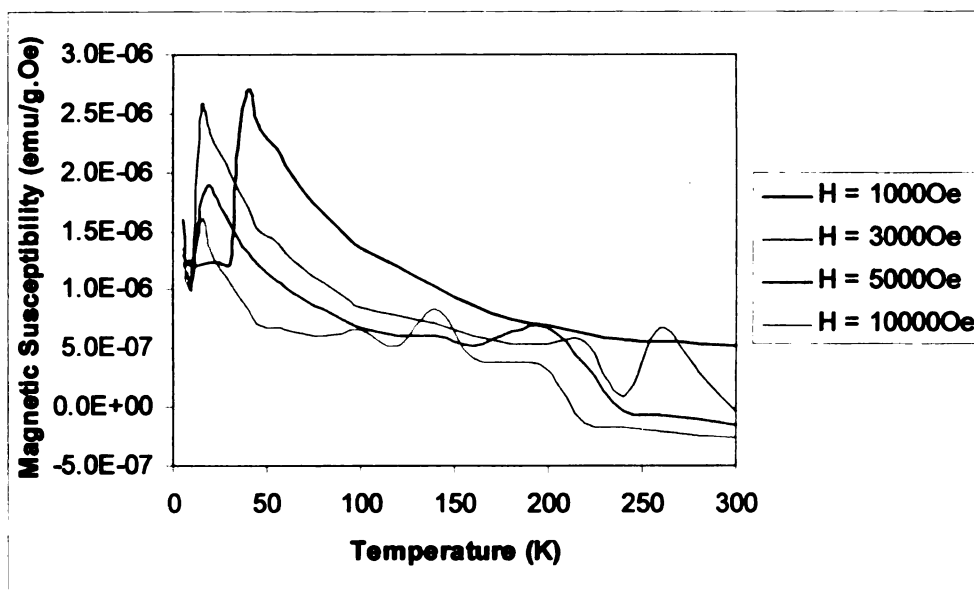
As shown in Figure 3.8-(b), The classical saturation curve for the paramagnetic component is evident for the 5 K measurement. The paramagnetic component is not as evident at 300 K because of thermal randomization leading to domination by the diamagnetic polymer background at higher field. An important feature of these measurements is the presence of a bell shaped peak between 1800 and 3200 Oe. The position is temperature independent but it is much more prominent at low temperature as judged by the intensity of the peak for the 5 K curve. This suggests the formation of a field-induced but highly magnetic phase that is a special point on the temperature-field-magnetization landscape.



(a)



(b)

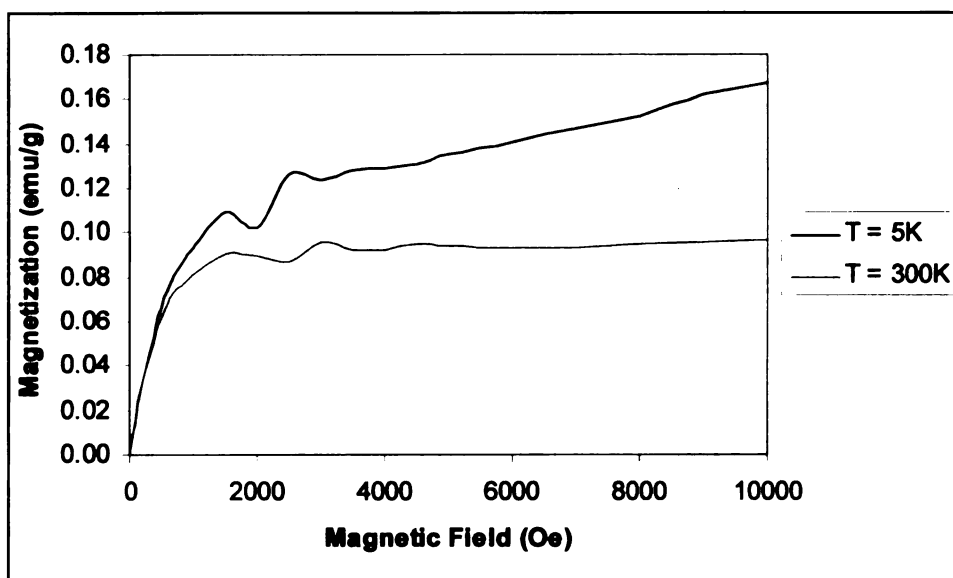


(c)

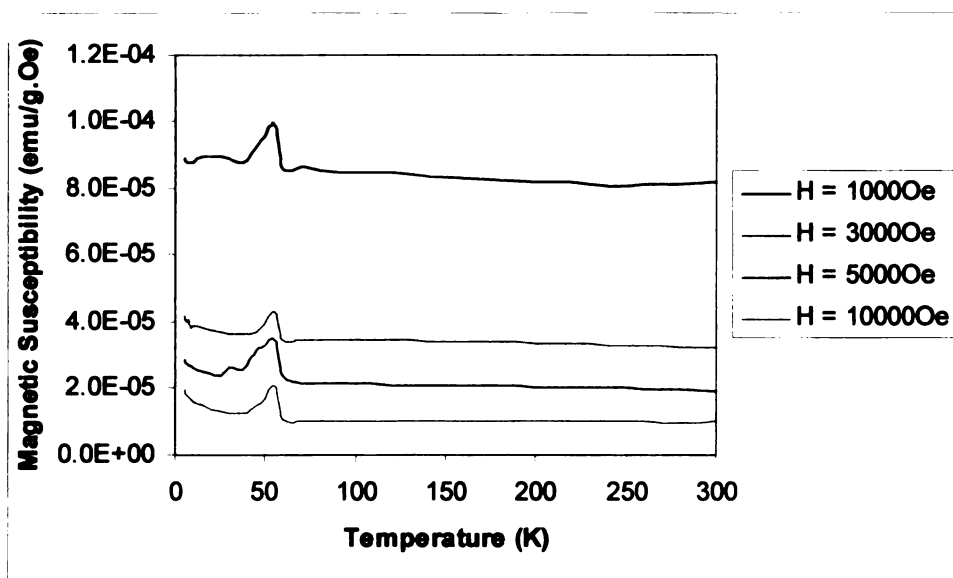
**Figure 3.8.** Magnetic properties of high MW poly(glycidyl pentafluorophenyl ether) doped with 20 wt % potassium. (a): Field dependence of magnetization at specific temperatures ; (b): Field dependence of mass susceptibility at specific temperatures; (c): Temperature dependence of mass susceptibility at specific fields.

Figure 3.9 shows the field dependence of the magnetization ( $M$ ) and the temperature dependence of the mass susceptibility ( $\chi_g$ ) of high MW poly(glycidyl pentafluorophenyl ether) doped with 30 weight % sodium. This material exhibits paramagnetic properties at the temperature range 5-35K. At 35-55K, a sharp increase in measured susceptibility is indicative of the onset of antiferromagnetic coupling. At higher temperatures (60-300K), the material becomes paramagnetic again.





(a)



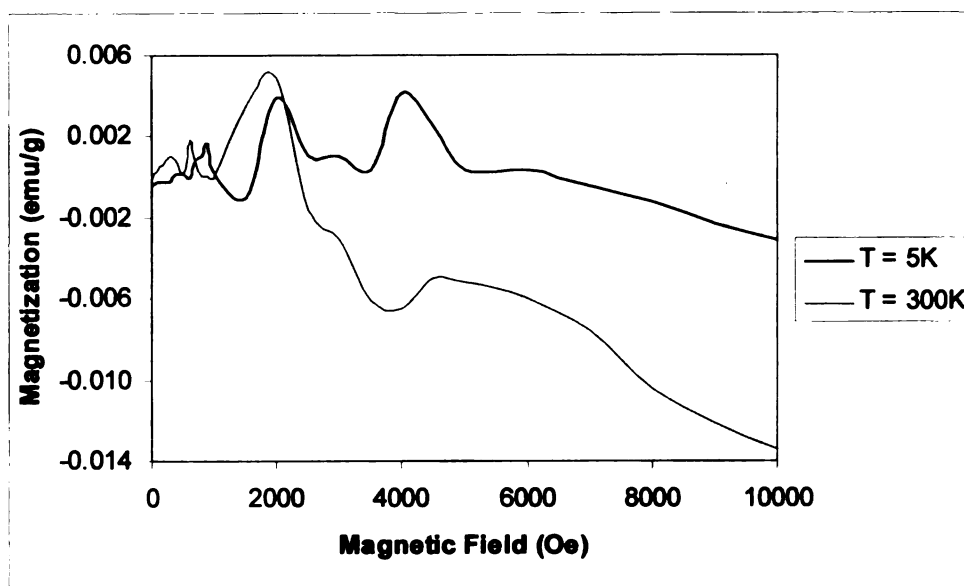
(b)

**Figure 3.9.** Magnetic properties of high MW poly(glycidyl pentafluorophenyl ether) doped with 30 wt % sodium. (a): Field dependence of magnetization at specific temperatures; (b): Temperature dependence of mass susceptibility at specific fields.

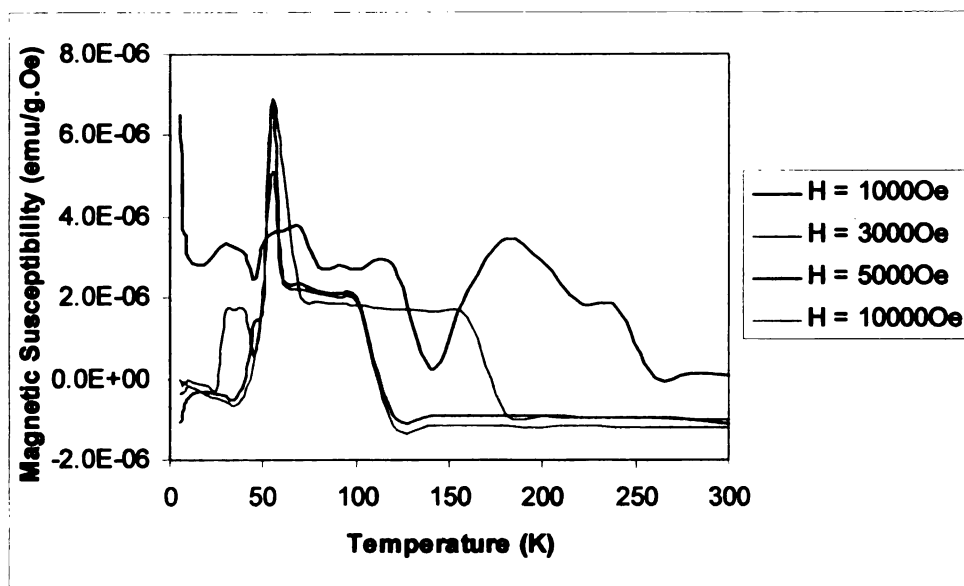
Normally the magnetic moments coupling occurs in some typical regions (called domain) instead of through out the entire material. The material may contain several different domains in which different types of coupling presents. In this case the observed magnetic properties may be complex due to the overall effect of difference types of magnetic states. The magnetic properties of high MW poly(glycidyl pentafluorophenyl ether) doped with 22 weight % sodium is an example, as shown in Figure 3.10.

The temperature at the Neel point was a function of the metal used and the field. Generally, metallation with sodium gave products that displayed Neel points at 35 to 40 degrees higher than materials doped with potassium. Thus metallation with potassium produced softer phases.

Figure 3.11 and Figure 3.12 show the magnetic properties of medium MW(2000-10000) poly(glycidyl pentafluorophenyl ether) doped with 25 wt % potassium and 35 wt % sodium respectively.

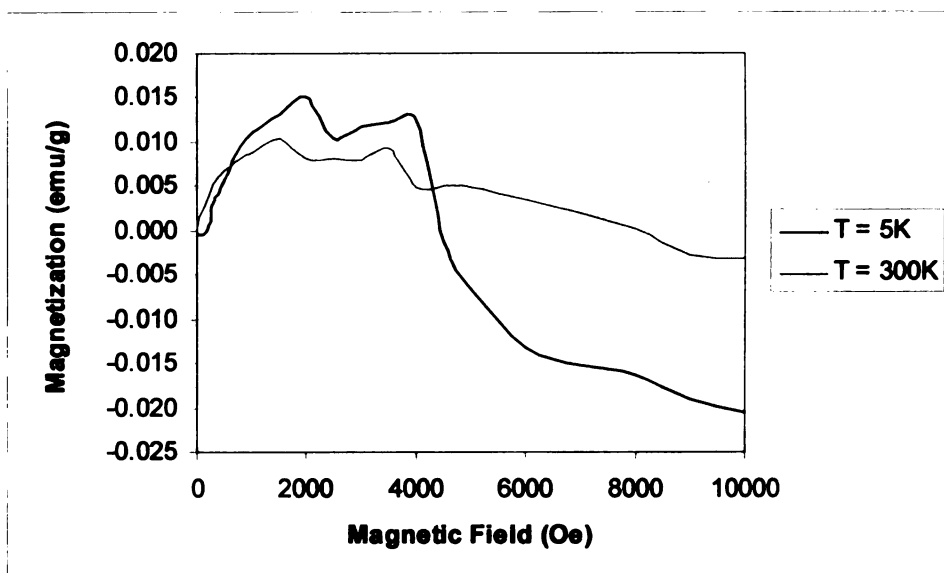


(a)

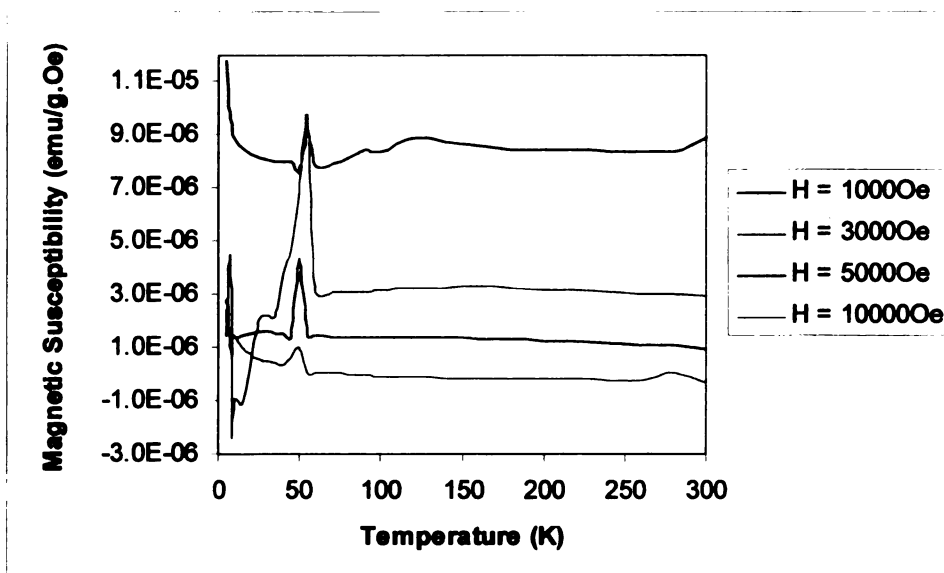


(b)

**Figure 3.10.** Magnetic properties of high MW poly(glycidyl pentafluorophenyl ether) doped with 22 wt % sodium. (a): Field dependence of magnetization at specific temperatures; (b): Temperature dependence of mass susceptibility at specific fields.

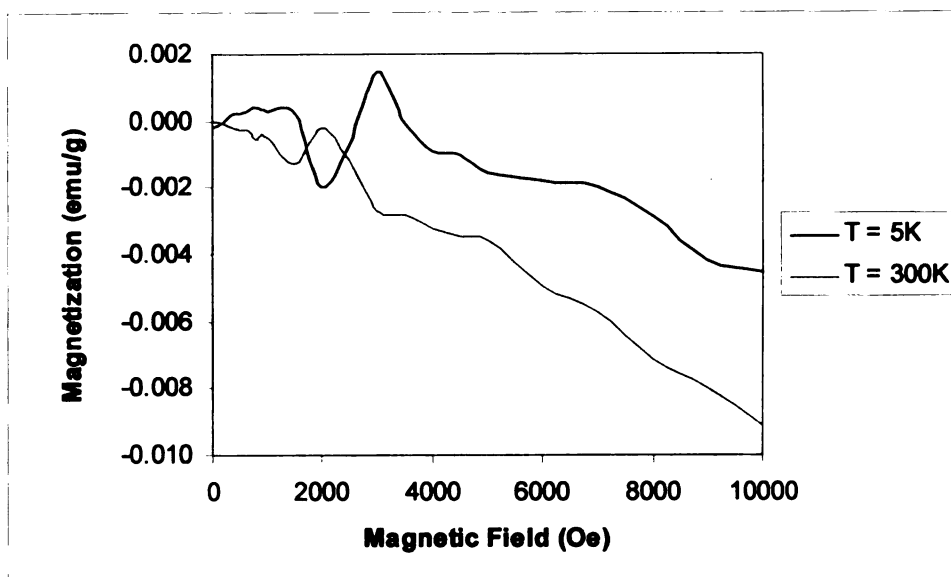


(a)

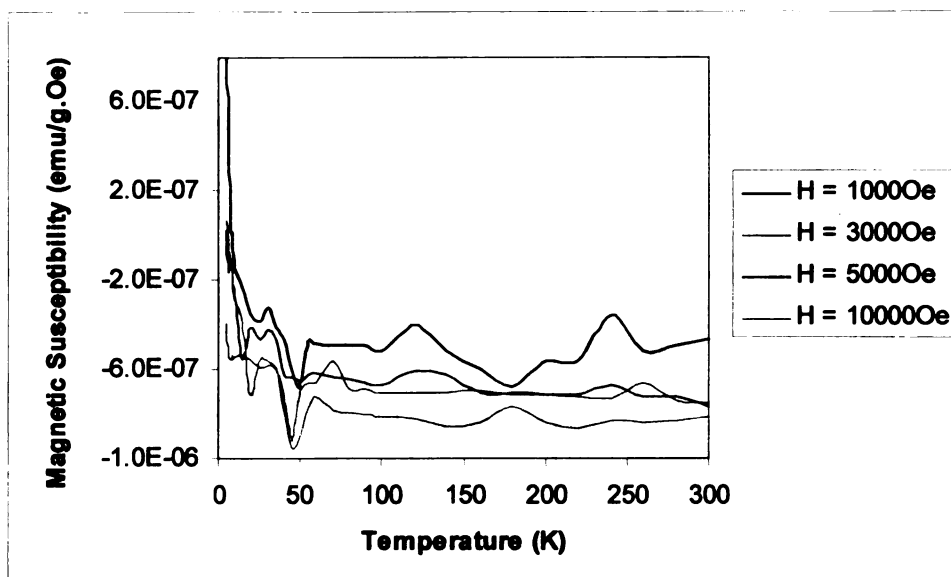


(b)

**Figure 3.11.** Magnetic properties of medium MW poly(glycidyl pentafluorophenyl ether) doped with 25 wt % potassium. (a): Field dependence of magnetization at specific temperatures; (b): Temperature dependence of mass susceptibility at specific fields.



(a)



(b)

**Figure 3.12.** Magnetic properties of medium MW poly(glycidyl pentafluorophenyl ether) doped with 35 wt % sodium. (a): Field dependence of magnetization at specific temperatures; (b): Temperature dependence of mass susceptibility at specific fields.

### 3.3.3.3. Conductivity Measurements

The doped poly(glycidyl pentafluorophenyl ether) was dissolved in THF to get a series of solutions with different concentrations. The dc electrical resistance of these solutions was measured at room temperature. The data are shown in Table 3.2. The resistance of the doped polymer varies strongly with the length of the polymer chain, the doped high MW polymers show much smaller resistance than the doped oligomers. Difference in the concentration of the THF solutions has a much smaller influence. These measurements indicated that the materials were essentially insulators at room temperature.

**Table 3.2.** The room-temperature dc electrical resistance of doped poly(glycidyl pentafluorophenyl ether) in THF.

Material: poly(glycidyl pentafluorophenyl ether) doped with alkali metals	Doping level: wt % of metals in the polymer	Resistance (M $\Omega$ )
High MW fraction doped with potassium	22.5 %	2-4
Oligomers doped with potassium	20.1 %	10-12
High MW fraction doped with sodium	22.2 %	5-8
Oligomers doped with sodium	6.3 %	10-11
High MW fraction doped with lithium and potassium	25.2 %	0.3-0.4
Oligomers doped with lithium and potassium	2.6 %	8-9

### 3.3.3.4. EPR Analysis

Electronic structure is an important concept in chemistry. EPR is a sensitive tool to study molecular structure, order, and dynamics of systems with unpaired electron spins. EPR (Electron Paramagnetic Resonance), often called ESR (Electron Spin Resonance), is a branch of spectroscopy in which electromagnetic radiation is absorbed by molecules, ions, or atoms possessing electrons with unpaired spins, i.e. electronic spin  $S > 0$ . EPR is similar to NMR (Nuclear Magnetic Resonance) which deals with nonzero nuclear spins,  $I > 0$ . In both EPR and NMR, the sample material is immersed in a strong static magnetic field and exposed to an orthogonal low-amplitude high-frequency field. ESR usually requires microwave-frequency radiation (GHz), while NMR is observed at low radio frequencies (MHz). The typical mode of EPR signal detection is: microwave frequency is kept constant and magnetic field is varied. There is a characteristic magnetic field where energy is absorbed by the sample when the frequency of the radiation is appropriate to the energy separation between two different electron spin states in the sample.

Most of the materials in a bulk form at normal conditions have net zero electronic spin and, thus, are EPR silent, but some can provide an EPR signal. The representative species are: Free radicals (highly reactive molecules which contain a single unpaired electron); Organic-ion radicals (very reactive species which are created along a course of redox reactions); Triplet-state organic molecules and biradicals; Transition-metal and rare-earth species which contain unpaired  $nd$  and/or  $mf$  electrons (e.g. iron, copper, cobalt).

Paramagnetic centers are created during doping of polymer materials. EPR spectroscopy is unique in the sense that it can specifically probe the paramagnetic molecules. Most paramagnetic metal centers require low (20K or lower) temperatures for detection.

Figure 3.13 shows the temperature dependence of the EPR spectra of high MW(10000-50000) poly(glycidyl pentafluorophenyl ether) doped with 40 wt% potassium. The spectra showed two overlapped signals with hyperfine splittings. The hyperfine structures are due to electrons trapped in the pentafluorophenyl groups and coupled with the fluorine atoms. The signal at lower field is assigned to the pentafluorophenyl radical anions and the signal at higher field is assigned to the itinerant electrons. In the low temperature region below 20K, the spectra are Dysonian in shape. The existence of an asymmetry of the EPR spectra characterized by  $A/B > 1$  (A and B are the amplitude of the low field and high field peaks respectively of the EPR derivative), is a direct consequence of the high conductivity of the material.<sup>20</sup> At higher temperature (20K-80K), the EPR line shape becomes more symmetrical, indicating a decrease of the conductivity. The integrated intensity of the signal decreases with increasing temperature over a wide range from 4K to 100K and this change of EPR intensity was found to be reversible against the temperature.



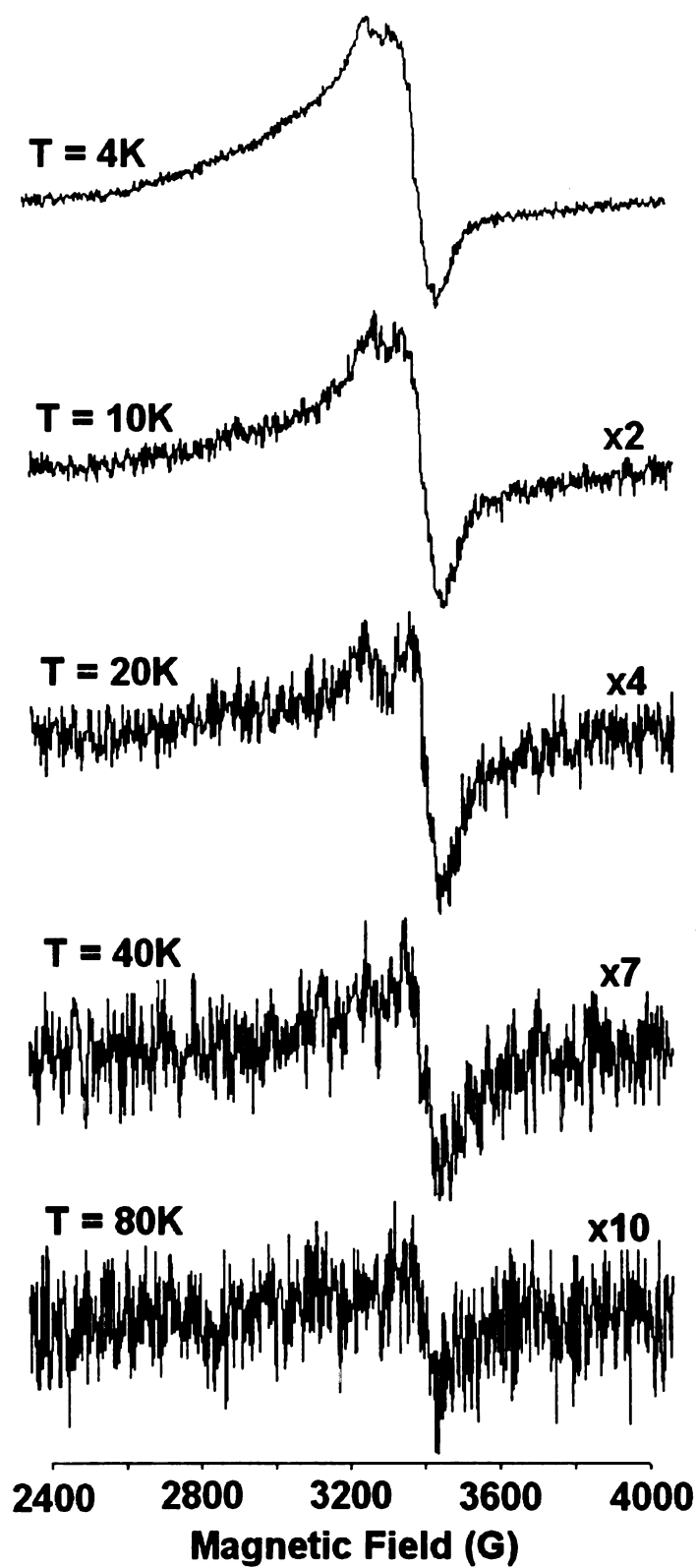


**Figure 3.13.** EPR spectra of high MW poly(glycidyl pentafluorophenyl ether) doped with 40 wt % potassium at different temperatures.

### 3.4. References

1. Ulrich Sowada and Richard A. Holroyd. *J. Phys. Chem.* **1980**, 84, 1150-1154.
2. Lajos Nyikos, Cornelis A. M. van den Ende, John M. Warman and Andries Hummel. *J. Phys. Chem.* **1980**, 84, 1154-1155.
3. Cornelis A. M. van den Ende, Lajos Nyikos, John M. Warman and Andries Hummel. *Radiat. Phys. Chem.* **1982**, 19, 297-308.
4. L. N. Shchegoleva, I. V. Beregovaya and P. V. Schastnev. *Chemical Physics Letters* **1999**, 312, 325-332.
5. I. V. Beregovaya and L. N. Shchegoleva. *International Journal of Quantum Chemistry* **2002**, 88, 481-488.
6. D.V. Stass, N.N. Lukzen, B. M. Tadjikov, V. M. Grigoryantz and Yu. N. Molin. *Chemical Physics Letters* **1995**, 243, 533-539.
7. T. Oomori and T. Hikida. *Chemical Physics* **1993**, 178, 477-481.
8. H. Faidas, L. G. Christophorou and D. L. McCorkle. *Chemical Physics Letters* **1992**, 193, 487-492.
9. K. S. Gant and L. G. Christophorou. *The Journal of Chemical Physics* **1976**, 65, 2977-2981.
10. Matsuura, H., Fukuhara, K.J. *Mol Struct.* **1985**, 126, 251.
11. Bjorling M., Karlstrom G. and Linse P. *J. Phys. Chem.* **1991**, 95, 6706-6709.
12. Maryno, Toru; Sasaki, Shigekuni; Nakamura, Kozaburo. Jpn. Kokai Tokkyo Koho. **1985**. Patent No.: JP 60224680 A2 19851109 Showa. Application No.: JP 84-80134 19840423.
13. P. Brūzga, J.V. Gražulevičius and R. Kavaliūnas. *Eur. Polym. J.* **1991**, 27, 707-711.
14. Tatsuya Toneri, Ken-ichi Watanabe, Fumio Sanda, and Takeshi Endo. *Macromolecules* **1999**, 32, 1293-1296.
15. Takuzo Aida, Yasunari Maekawa, Shoichi Asano, and Shohei Inoue. *Macromolecules* **1988**, 21, 1195-1202.
16. Tomokazu Yasuda, Takuzo Aida, and Shohei Inoue. *Bull. Chem.Soc. Jpn.* **1986**, 59, 3931-3934.

17. Keiichi Takuma, Toshikazu Takata, and Takeshi Endo. *Macromolecules* **1993**, 26, 862-863.
18. Charles C. Price and Murali Krishna Akkapeddi. *J. Amer. Chem. Soc.* **1972**, 3972-3975.
19. Cornelis A. M. van den Ende, Lajos Nyikos, John M. Warman and Andries Hummel. *Radiat. Phys. Chem.* **1982**, 19, 297-308.
20. P. Bernier, A. El-Khodary, F. Rachdi and C. Fite. *Synthetic Metals* **1987**, 17, 413-417.

### 3.5. Conclusions

Poly(glycidyl pentafluorophenyl ether), a polyethylene oxide type material containing a pentafluorophenoxymethyl substituent on each ethylene fragment was prepared and used as a matrix for the dissociative solvation of the alkaline metals potassium and sodium. Systems in which the metal cations are stabilized by the polyether system and the electrons are captured by the pentafluorophenyl group to form highly colored (pink to violet) anionic bands were formed. Condensed phase systems containing high densities of aromatic radical anions forming delocalized electronic bands hold special promise. Depending on the clustering of energy states, might behave as semiconductors under some temperature regimes. They may behave as superconductors in other temperature domains. Such materials might have useful photochromic or electrochromic or other optical-electronic properties. The optical, magnetic and electronic properties of the systems were examined by UV-visible spectroscopy, variable temperature electron paramagnetic resonance (EPR) spectroscopy and magnetometry using a superconducting quantum interference device (SQUID). The new materials are antiferromagnetic with some paramagnetic domains. They displayed highly asymmetric (Dysonian) EPR first derivative curves in the temperature range of 4 – 80 K indicating the presence of very highly conductive states in these regimes. Unlike the alkali metal and electride systems described before, the new systems we describe here are stable for several months at room temperature and do not ignite spontaneously in air. Such stability is not known in alkali metal / organic systems. This greatly increases the potential for use of the materials described here in device fabrication.

**Chapter 4. Synthesis and Characterization of the Doped**  
**Poly[penta(ethylene glycol) dinitrobenzoyl ether] and**  
**Poly[penta(ethylene glycol) pentafluorophenyl ether]**

We also synthesized other two polyether-based polymers containing nitrobenzoyl and pentafluorobenzyl groups respectively.

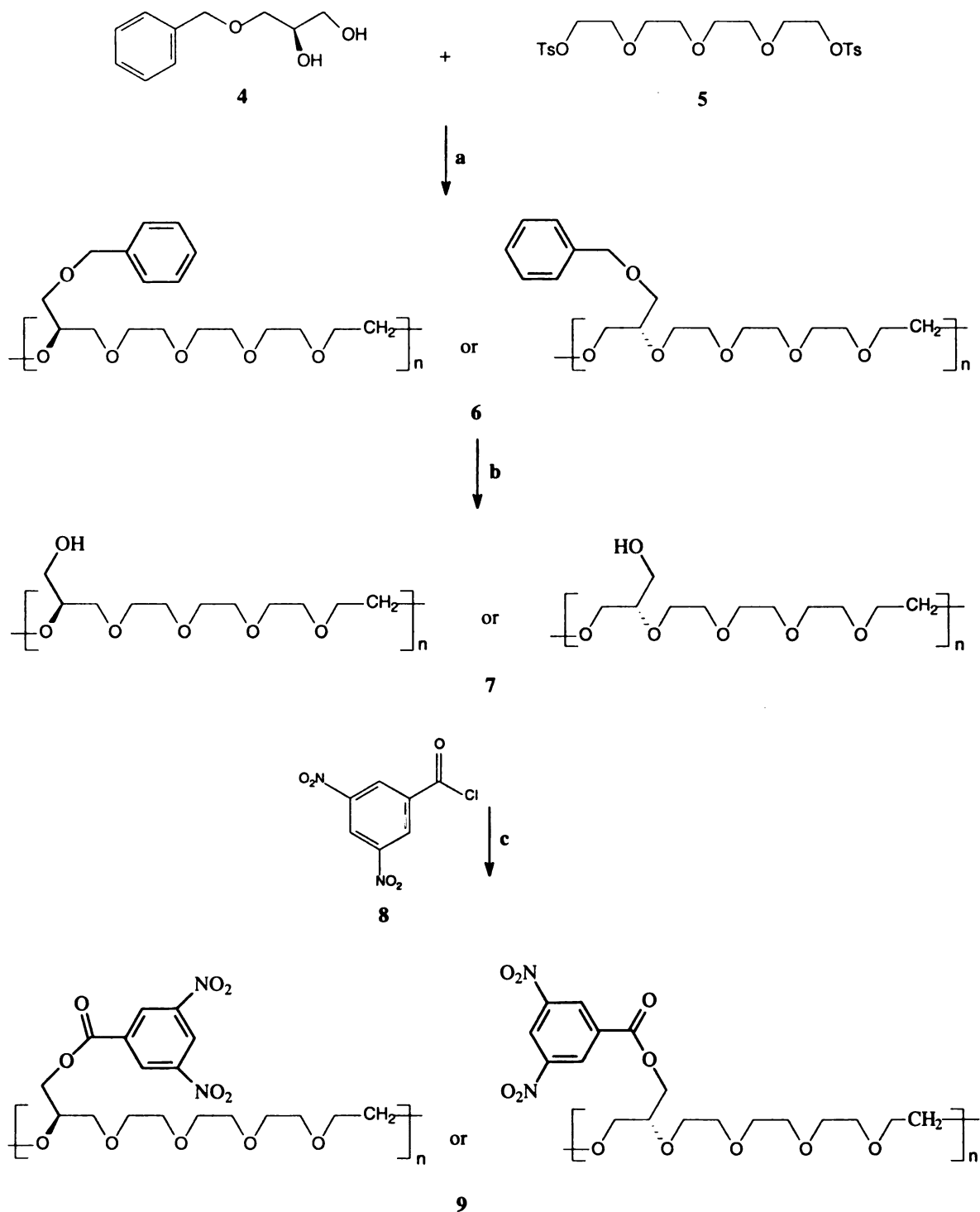
## **4.1. Experimental**

### **4.1.1. Synthesis of Poly[penta(ethylene glycol) dinitrobenzoyl ether]**

All chemicals were used as received from Aldrich unless otherwise noted. (R)-(+)-1-benzylglycerol was purchased from Acros Organics.

The route to poly[penta(ethylene glycol) dinitrobenzoyl ether] is outlined in Scheme 4.1.

**Scheme 4.1** Synthesis of poly[penta(ethylene glycol) dinitrobenzoyl ether]



Reagents and conditions: (a) NaH, THF, reflux (80°C), 24h; (b) hydrogen, 10% Pd-C, ethanol, 25°C, 48h, 95%; (c) pyridine, 25°C, 24h.

**(a). Preparation of poly[penta(ethylene glycol) benzylic ether]**

The mole ratio of the starting materials was: compound **4**/compound **5**/sodium hydride = 1.0/1.0/3.0. 0.016mol sodium hydride was washed by 50ml hexanes before use. 0.0055mol (R)-(+)-1-benzylglycerol (compound **4**) was dissolved in 10ml THF and added to the sodium hydride at 0°C. The solution of 0.0055mol tetra(ethylene glycol) di-p-tosylate (compound **5**) in 15ml THF was then slowly added through a dropping funnel. There was rapid evolution of hydrogen and the reaction mixture became viscous. The temperature was increased and the mixture was refluxed for 24h. After the reaction was done, the solution was stripped of THF and 200ml 2:1 CHCl<sub>3</sub>/H<sub>2</sub>O was added. TsONa was dissolved in water while most of the product was in the organic layer. The solvent was removed under reduced pressure to give polymer **6**, which is yellow sticky liquid.

**(b). Deprotection of poly[penta(ethylene glycol) benzylic ether]**

Polymer **6** was diluted in ethanol to form a 10% solution. The amount of catalyst used was: 10% Pd-C/polymer **6** = 5 weight %. The pressure of hydrogen was 20 psi. The reaction mixture was stirred at r.t. for 48h to give the reduction product (polymer **7**) in high yield. It was very important to remove any ethanol from the product before the following esterification step.



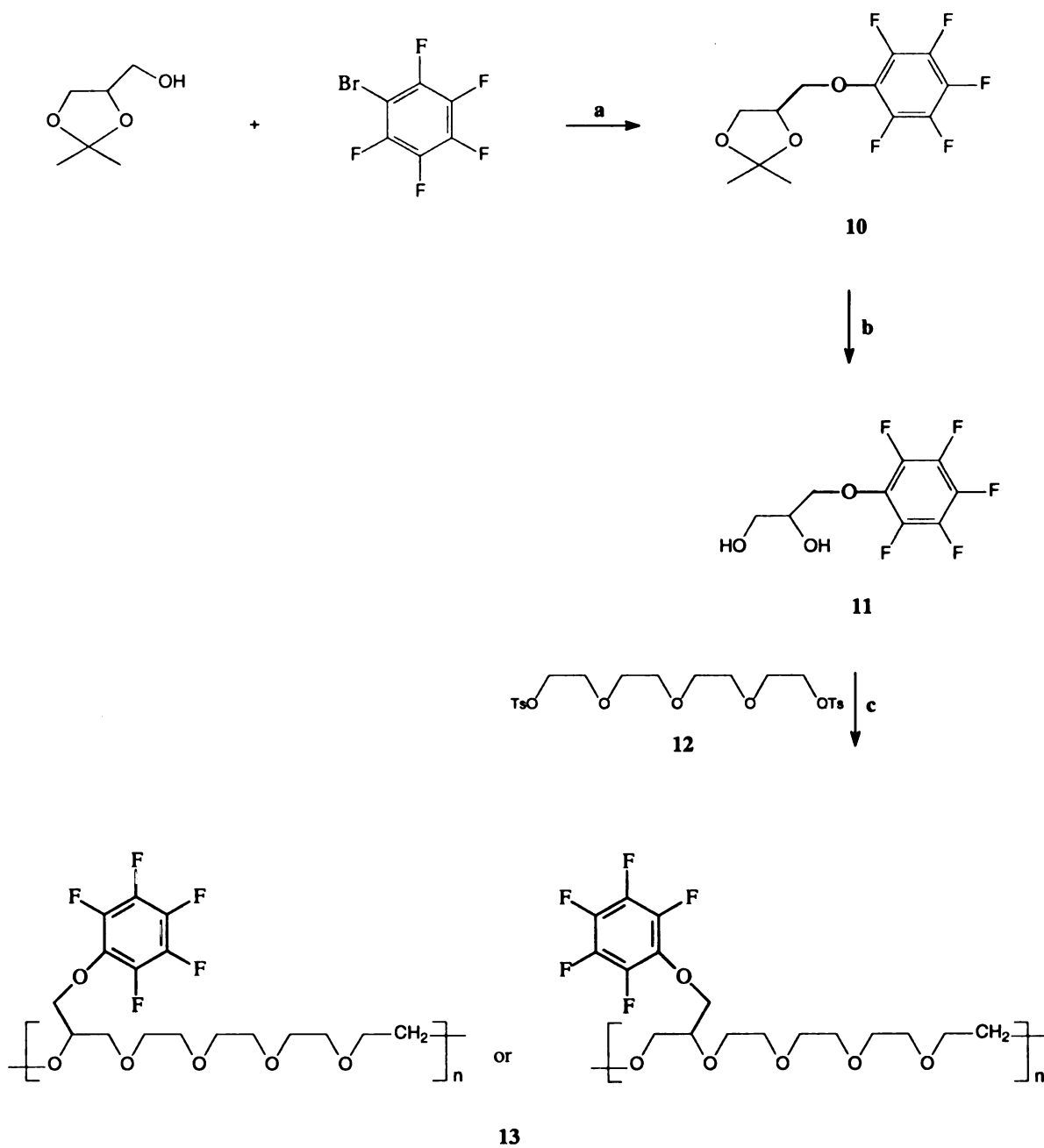
### **(c). Preparation of poly[penta(ethylene glycol) dinitrobenzoyl ether]**

The mole ratio of the starting materials was: polymer 7/3,5-dinitrobenzoyl chloride = 1.0/1.2. The reaction was carried out in pyridine at r.t.. Polymer **9** is soluble in chloroform while excess 3,5-dinitrobenzoyl chloride has very low solubility and therefore can be easily filtered off from the chloroform layer. Polymer **9** was then purified by gel permeation chromatography (GPC) using “Sephadex LH-20” gel. The molecular weight (MW) was estimated by HPLC using “Shodex Asahipak GS-310 7G” column and THF as eluant.

### **4.1.2. Synthesis of Poly[penta(ethylene glycol) pentafluorophenyl ether]**

The route to poly[penta(ethylene glycol) pentafluorophenyl ether] is outlined in Scheme 4.2.

**Scheme 4.2** Synthesis of poly[penta(ethylene glycol) pentafluorophenyl ether]



**Reagents and conditions:** (a) NaH, THF, 0°C- r.t., 12h; (b) HCOOH, HCl, ethanol, reflux (80°C), 24h; (c) NaH, THF, reflux (70°C), 24h.

**(a). Preparation of (2,2-dimethyl-1,3-dioxolane-4-methanol) pentafluorophenyl ether**

The first step of the synthesis is a  $S_N2$  reaction between commercially available solketal (2,2-dimethyl-1,3-dioxolane-4-methanol) and bromopentafluorobenzene in THF. The mole ratio of the starting materials was: solketal/bromopentafluorobenzene/sodium hydride = 1.0/1.0/1.2. 5.1g 60% sodium hydride was washed by 200ml hexanes before use. The round bottom flask containing sodium hydride and 500ml THF was cooled in ice and solketal was added all at once while stirring, then bromopentafluorobenzene was added slowly over a period of 30min. The ice bath was removed and the reaction mixture stirred at r.t. for 12h. After the reaction was done, excess sodium hydride was destroyed by addition of ethanol. The reaction mixture was stripped of solvent and then 200ml 2:1  $CH_2Cl_2/H_2O$  was added. The organic layer was dried and condensed to give the orange colored compound **10**.

**(b). Hydrolysis of (2,2-dimethyl-1,3-dioxolane-4-methanol) pentafluorophenyl ether**

88% formic acid was added to a 30% solution of compound **10** in ethanol. The reaction mixture was refluxed for 12h, then 1ml 36% hydrochloric acid was added and the solution was refluxed for another 12h. Some white deposit was formed which was readily soluble in water but was insoluble in ordinary organic solvents such as  $CHCl_3$  or DMSO. NMR analysis indicated that this white solid was not the product and was therefore filtered off from the reaction mixture. The filtrate was condensed and the crude

product was purified by flash column chromatography using 9:1 chloroform/ethyl acetate as the eluant.

#### **(c). Preparation of poly[penta(ethylene glycol) pentafluorophenyl ether]**

The mole ratio of the starting materials was: compound 11/compound 12/sodium hydride = 1.0/1.0/3.0. 1.2g 60% sodium hydride was washed with 50ml hexanes before use. Compound 11 was dissolved in 5ml THF and added to the mixture of sodium hydride in 15ml THF at 0°C. The solution of tetra(ethylene glycol)di-p-tosylate (compound 12) in 5ml THF was then added slowly through a dropping funnel. There was rapid evolution of hydrogen and the reaction mixture became viscous. The reaction mixture was then refluxed for 24h. The crude product was washed by water thoroughly to remove TsONa and then dried in air. Polymer 13 is pale yellow sticky solid, it doesn't melt at 250°C. Molecular weight (MW) of polymer 13 was estimated by HPLC using "Shodex Asahipak GS-310 7G" column and THF as the eluant. Some fraction of the polymer could not be dissolved in THF and was considered to have very high MW.

#### **4.1.3. Doping**

The experimental procedure of the doping step was the same as that described in Chapter 3.2.2.

## **4.2. Results and Discussion**

### **4.2.1. Characterization of the Undoped Polymers**

#### **4.2.1.1. Solubility**

Poly[penta(ethylene glycol) dinitrobenzoyl ether] exhibits good solubility in common organic solvents such as acetone, chloroform, dichloromethane, THF, DMF and DMSO at room temperature.

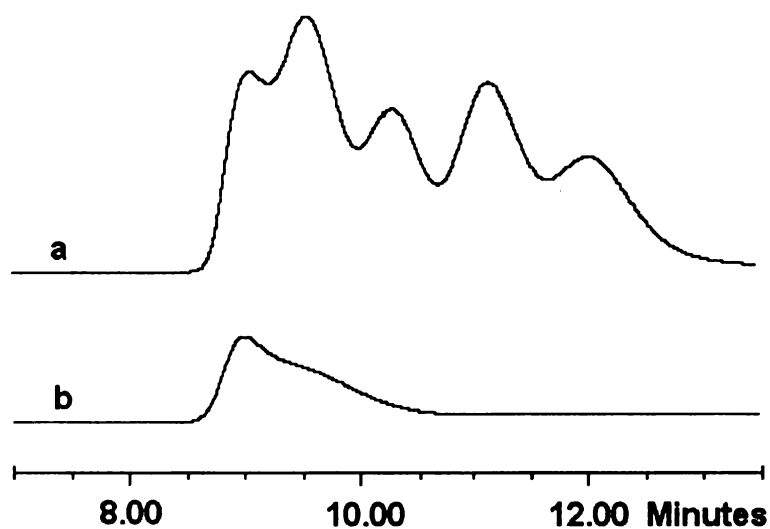
Poly[penta(ethylene glycol) pentafluorophenyl ether] is insoluble in acetone, ethanol, and DMSO; partially soluble in chloroform, dichloromethane, acetonitrile, ethyl acetate, THF and DMF at room temperature. Since the polymer shows limited solubility in common solvents, purification to remove the impurities or the trapped solvent was difficult even after vacuum drying.

#### **4.2.1.2. GPC Results**

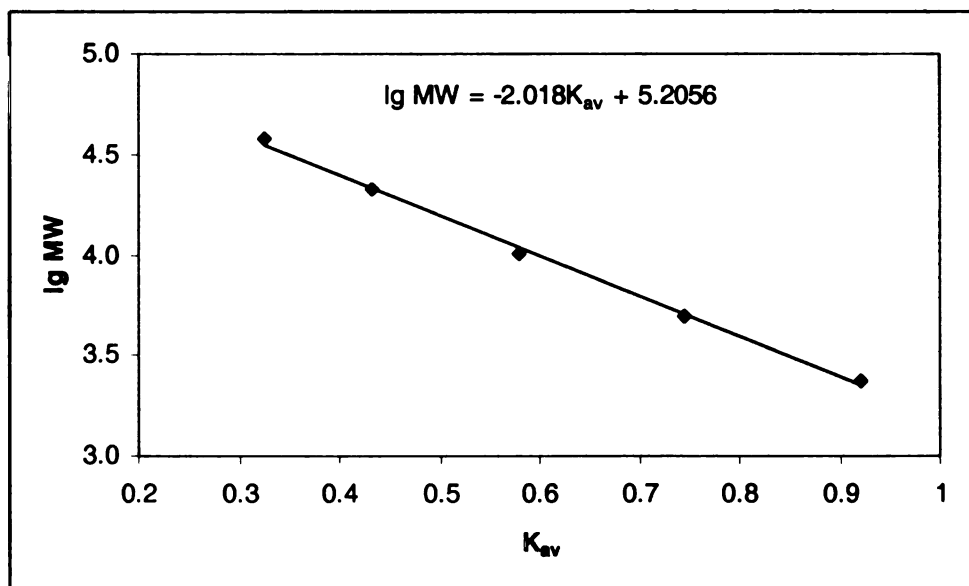
The molecular weight of these two polymers were measured by means of GPC using THF as eluant against polystyrene standards. The average molecular weight and the molecular weight distribution were calculated by means of standard curves shown in Figure 4.2 and Figure 4.4:  $K_{av} = (t_e - t_0)/(t_i - t_0)$  ;  $t_0 = 7.049\text{min}$  based on blue dextran;  $t_i = 12.058\text{min}$  based on glucose;  $t_e$  is the retention time of the measured polymer.

Figure 4.1-(b) shows the GPC results of poly[penta(ethylene glycol) dinitrobenzoyl ether]. The average molecular weight is 29721. The molecular weight distribution is 6500–42000.

Because poly[penta(ethylene glycol) pentafluorophenyl ether] is partially soluble in THF, only the THF-soluble fraction of the polymer was measured by GPC, the result is shown in Figure 4.3. The average molecular weight of the THF-soluble part was measured as 1666. It was not possible to determine the molecular weight of the insoluble fraction.



**Figure 4.1.** GPC chromatogram of (a) Polystyrene standards: MW = 38100, 21000, 10050, 4920, 2350; Retention time (min) = 8.675, 9.216, 9.950, 10.783, 11.665. (b) Poly[penta(ethylene glycol) dinitrobenzoyl ether]: Retention time = 8.870 min.



**Figure 4.2.**  $\lg MW$  v.s.  $K_{av}$  standard curve for poly[penta(ethylene glycol) dinitrobenzoyl ether].

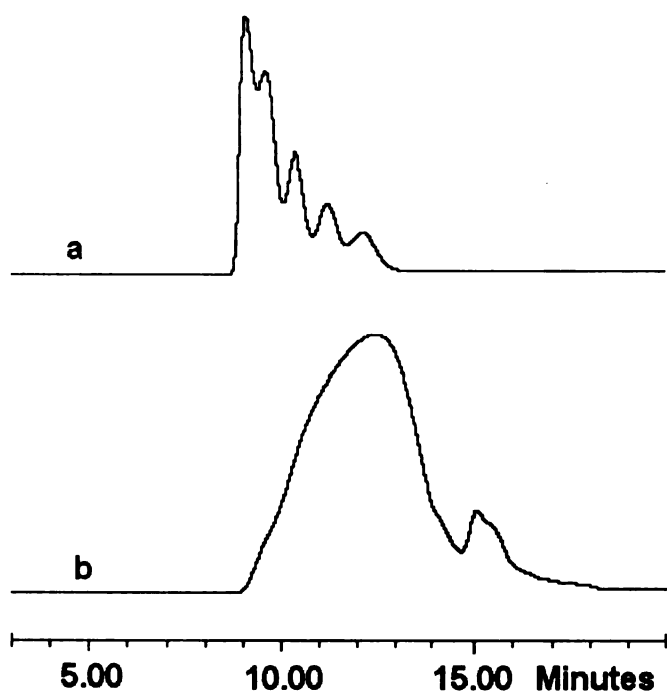


**Figure 4.3.** GPC chromatogram of (a) Polystyrene standards: MW = 38100, 21000, 10050, 4920, 2350; Retention time (min) = 8.707, 9.239, 9.975, 10.806, 11.686. (b) Poly[penta(ethylene glycol) pentafluorophenyl ether]: Retention time = 12 min.

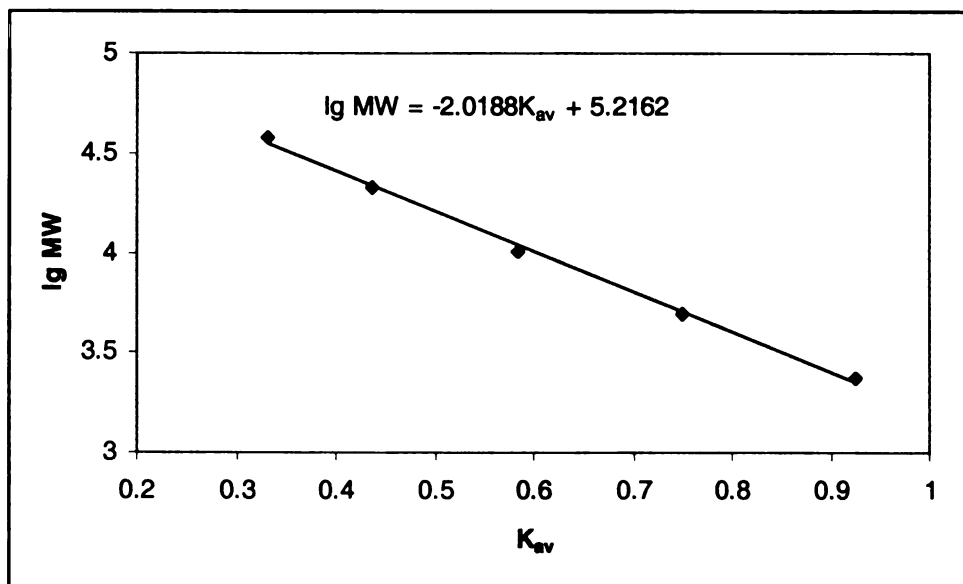


**Figure 4.4.**  $\lg MW$  v.s.  $K_{av}$  standard curve for poly[penta(ethylene glycol) pentafluorophenyl ether].



## 4.2.2. Characterization of the Doped Polymers

### 4.2.2.1. UV-visible Spectra

The UV-vis absorption spectra of the potassium doped poly[penta(ethylene glycol) dinitrobenzoyl ether] and poly[penta(ethylene glycol) pentafluorophenyl ether] are shown in Figure 4.5-(f) and (g). The density of pentafluorophenyl and nitrobenzoyl groups in these two polymers are much more lower compared with that of pentafluorophenyl groups in poly(glycidyl pentafluorophenyl ether), therefore no obvious absorption band is observed in the visible region.

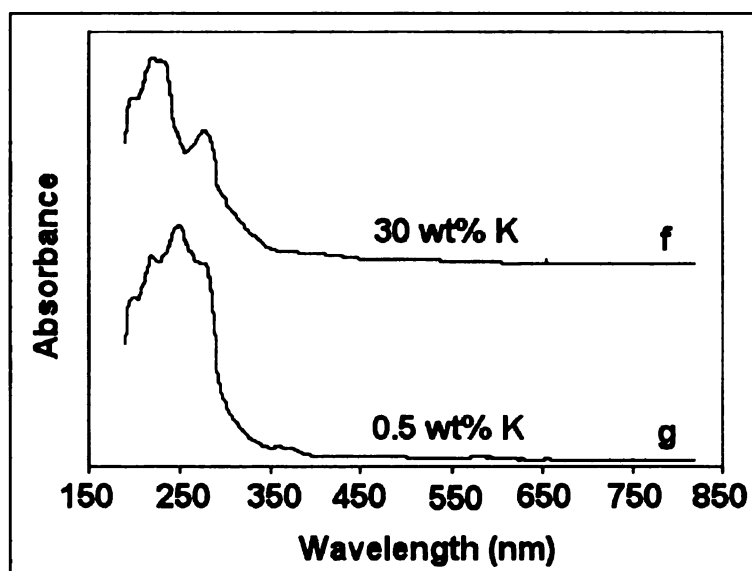
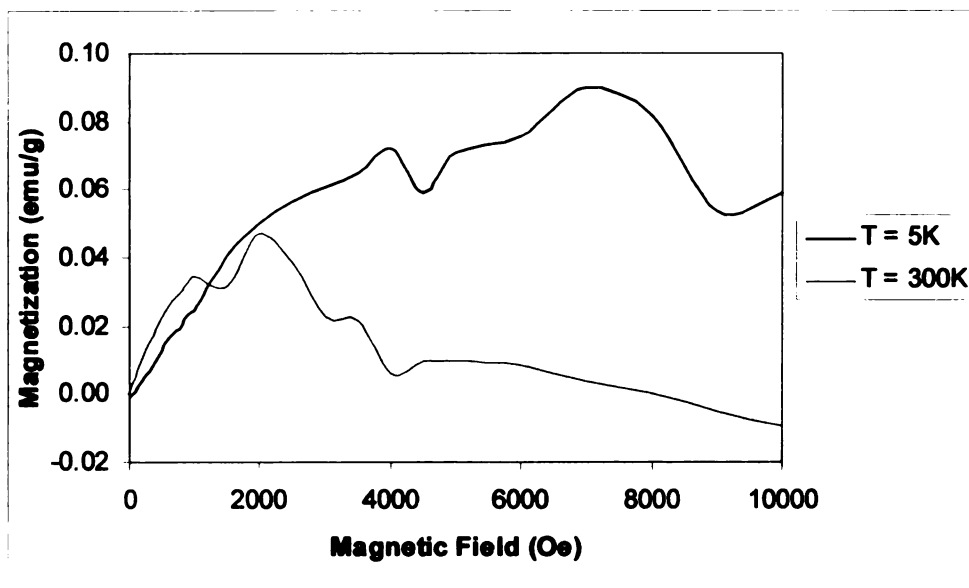


**Figure 4.5.** UV-vis absorption spectra of the doped polymers. (f): Poly[penta(ethylene glycol) dinitrobenzoyl ether]; (g): Poly[penta(ethylene glycol) pentafluorophenyl ether].

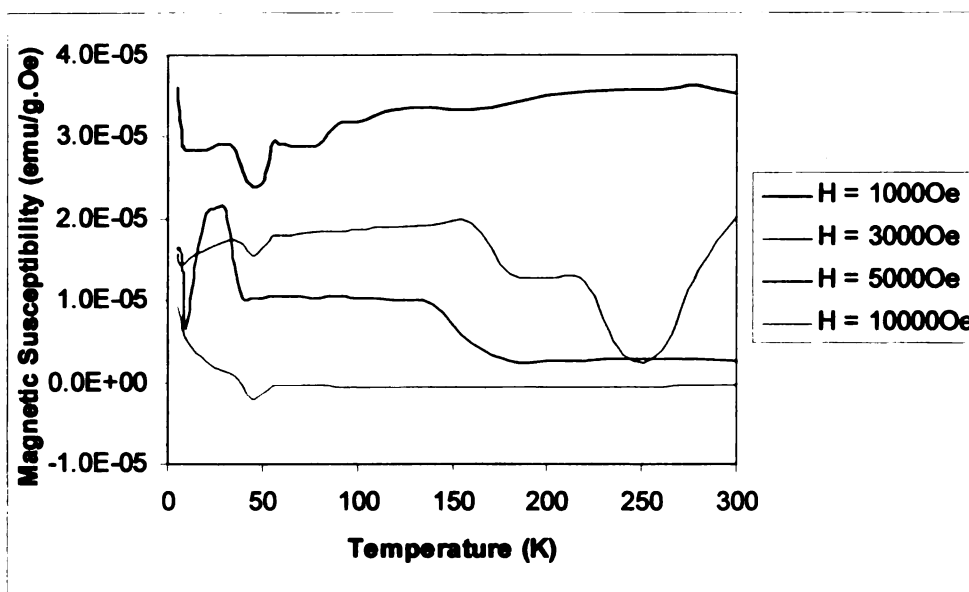
#### 4.2.2.2. Magnetic Properties

Figure 4.6 shows the field dependence of the magnetization ( $M$ ) and the temperature dependence of the mass susceptibility ( $\chi_g$ ) of poly[penta(ethylene glycol) dinitrobenzoyl ether] doped with 30 weight % potassium. When the external magnetic field is 5000Oe, the ferromagnetic coupling is observed at the temperature range 50-150K, the  $\chi_g$  value decreases with increasing temperature; at higher temperatures (150-300K), the magnetic susceptibility follows Curie-Weiss law for paramagnets; the Curie temperature ( $T_c$ ) is about 150K. When the external magnetic field is 10000Oe, this material exhibits paramagnetic properties at very low temperatures (5-50K); at the temperature range 50-300K, the material becomes weakly diamagnetic.

Figure 4.7 shows the field dependence of the magnetization ( $M$ ) and the temperature dependence of the mass susceptibility ( $\chi_g$ ) of poly[penta(ethylene glycol) pentafluorophenyl ether] doped with 0.5 weight % potassium. This material exhibits paramagnetic properties but there is appreciable curvature from the Curie-Weiss law.

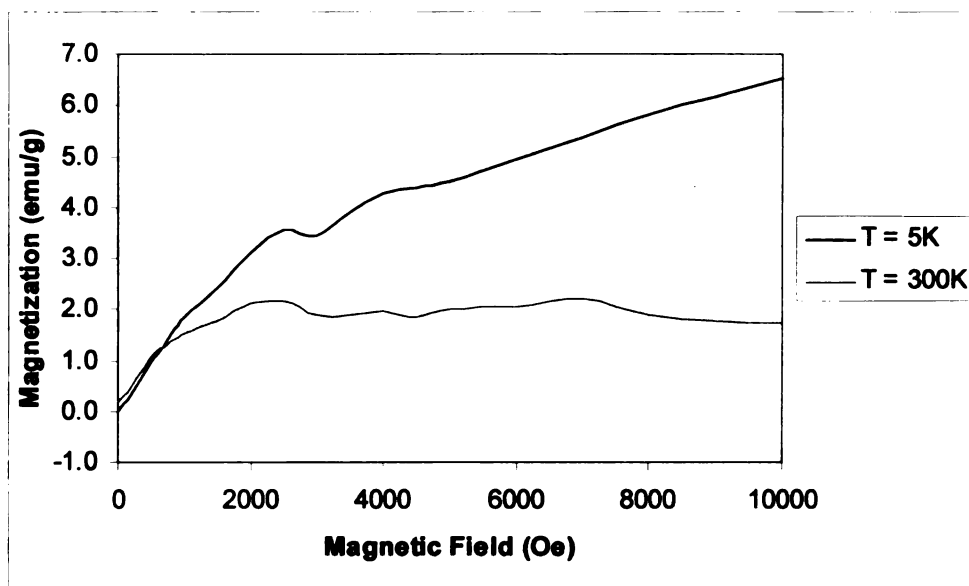


(a)

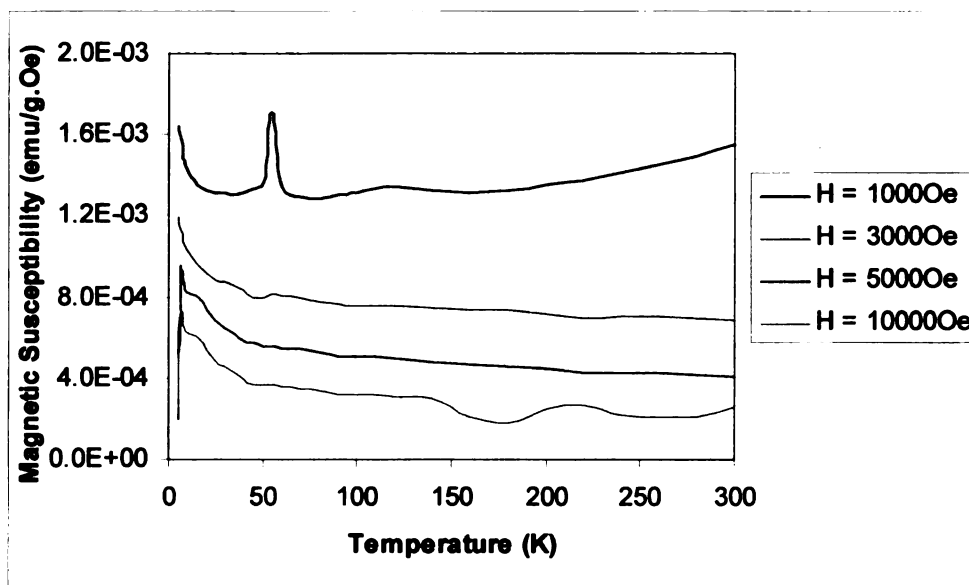


(b)

**Figure 4.6.** Magnetic properties of poly[penta(ethylene glycol) dinitrobenzoyl ether] doped with 30 wt % potassium. (a): Field dependence of magnetization at specific temperatures; (b): Temperature dependence of mass susceptibility at specific fields.



(a)



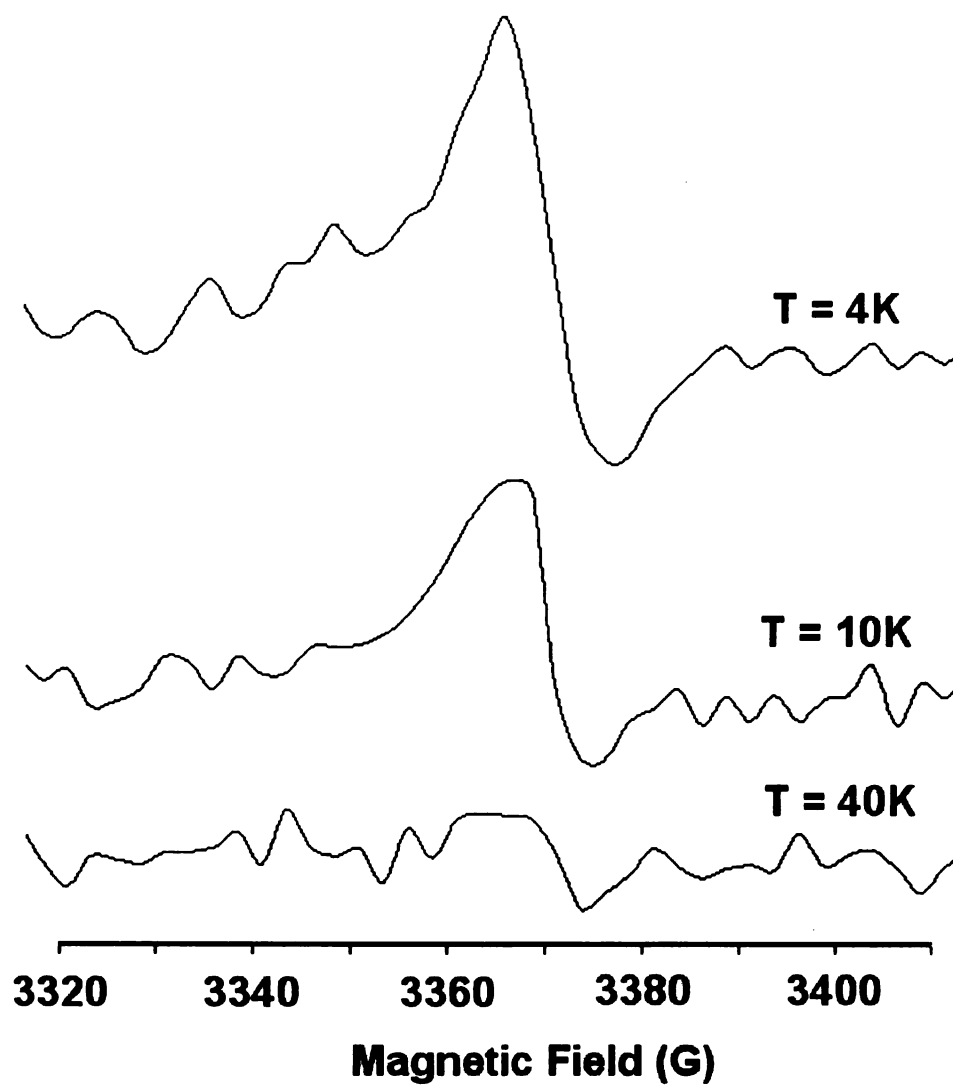
(b)

**Figure 4.7.** Magnetic properties of poly[penta(ethylene glycol) pentafluorophenyl ether] doped with 0.5 wt % potassium. (a): Field dependence of magnetization at specific temperatures; (b): Temperature dependence of mass susceptibility at specific fields.

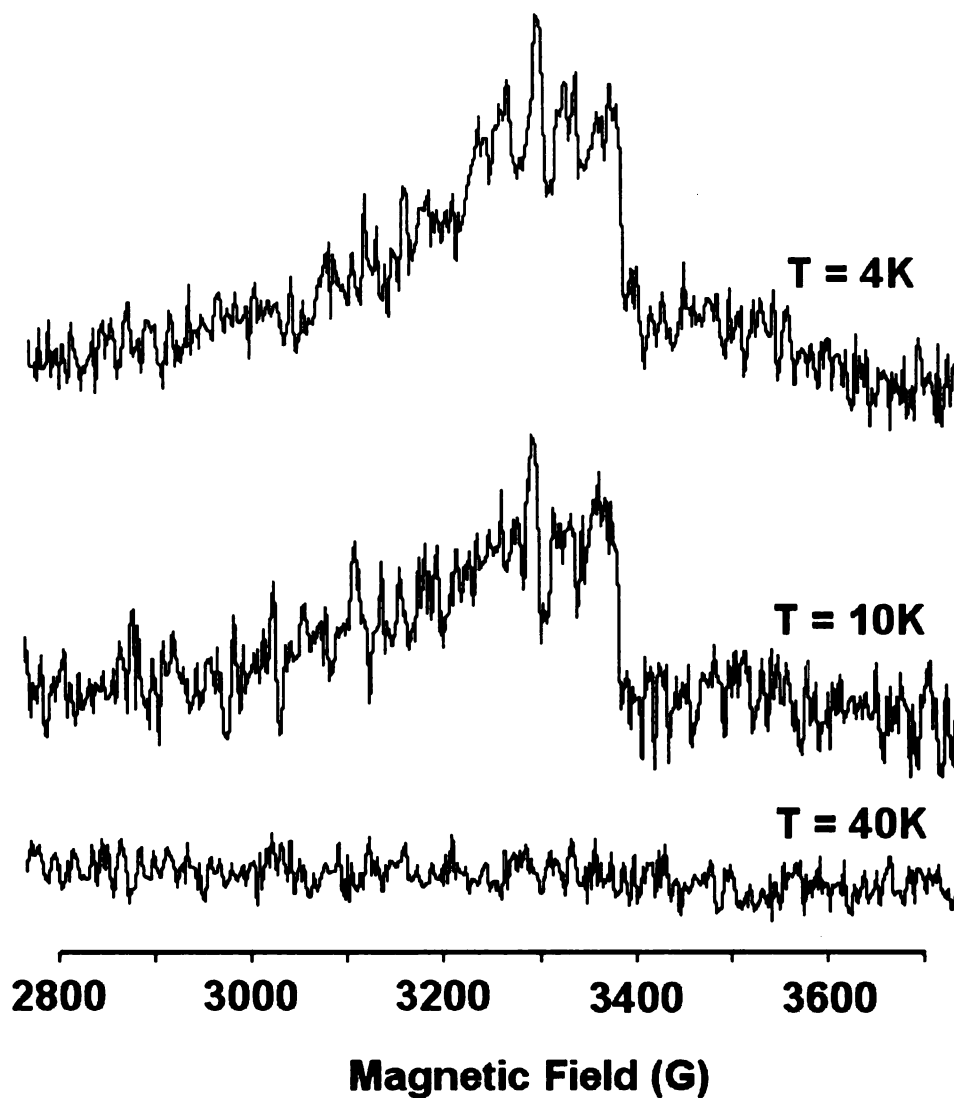
#### 4.2.2.3. EPR Analysis

Figure 4.8 shows the EPR spectra of poly[penta(ethylene glycol) dinitrobenzoyl ether] doped with 20 wt % potassium as a function of temperature from 4K-40K. The EPR spectrum consists of an unresolved line with line-width  $\Delta H_{pp} = 10G$ . Compared with the EPR spectra of poly(glycidyl pentafluorophenyl ether) doped with 40 wt % potassium, this observed narrower  $\Delta H_{pp}$  may be explained by the indirect exchange coupling between the localized spins via the itinerant electrons, resulting in an indirect exchange narrowing of the line.<sup>1</sup> The Dysonian line shape indicates the metallic behavior of this material at low temperature.

Figure 4.9 shows the temperature dependence of the EPR spectra of poly[penta(ethylene glycol) pentafluorophenyl ether] doped with 10 wt % potassium. The spectrum shows a broad single peak ( $\Delta H_{pp}$  is about 100G) with rather complicated hyperfine splittings due to spin coupling between the located electrons and the carbon atoms on the aromatic ring of the pentafluorophenyl groups. The spectral line shape is asymmetrical. The line absorption intensity decreases with temperature over the 4-40K range.



**Figure 4.8.** EPR spectra of poly[penta(ethylene glycol) dinitrobenzoyl ether] doped with 20 wt % potassium at different temperatures.



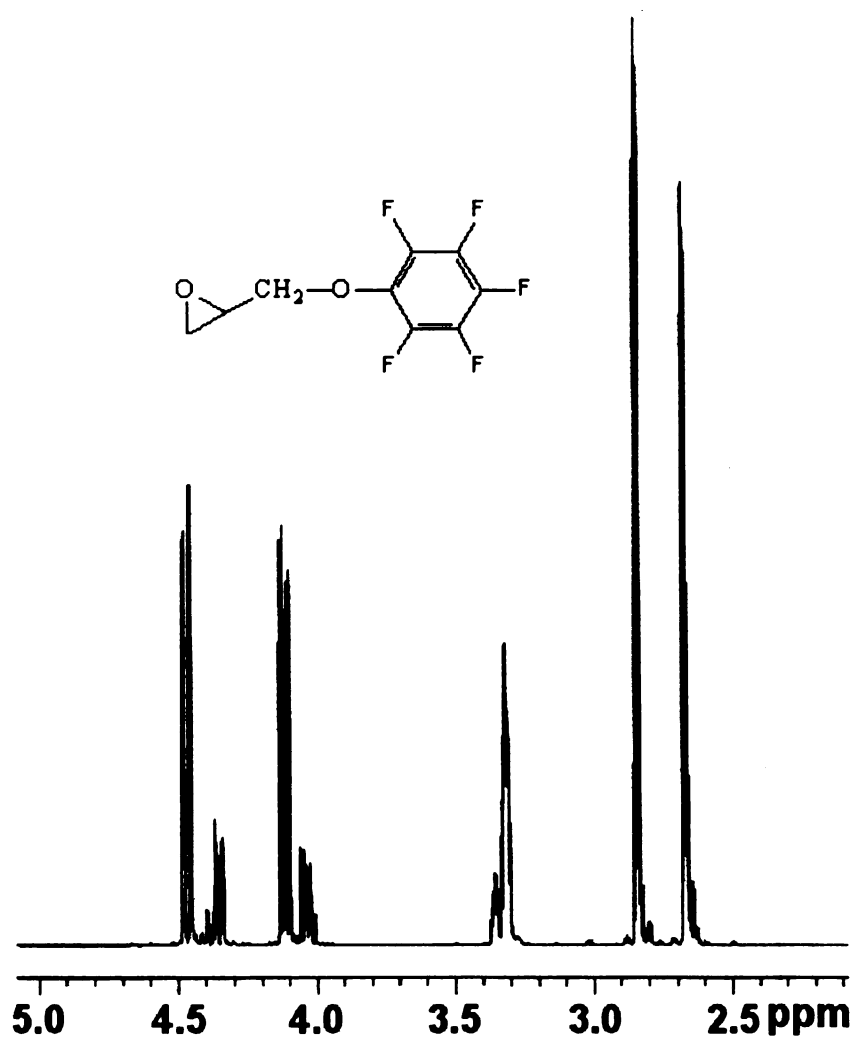
**Figure 4.9.** EPR spectra of poly[penta(ethylene glycol) pentafluorophenyl ether] doped with 10 wt % potassium at different temperatures.

#### 4.4. References

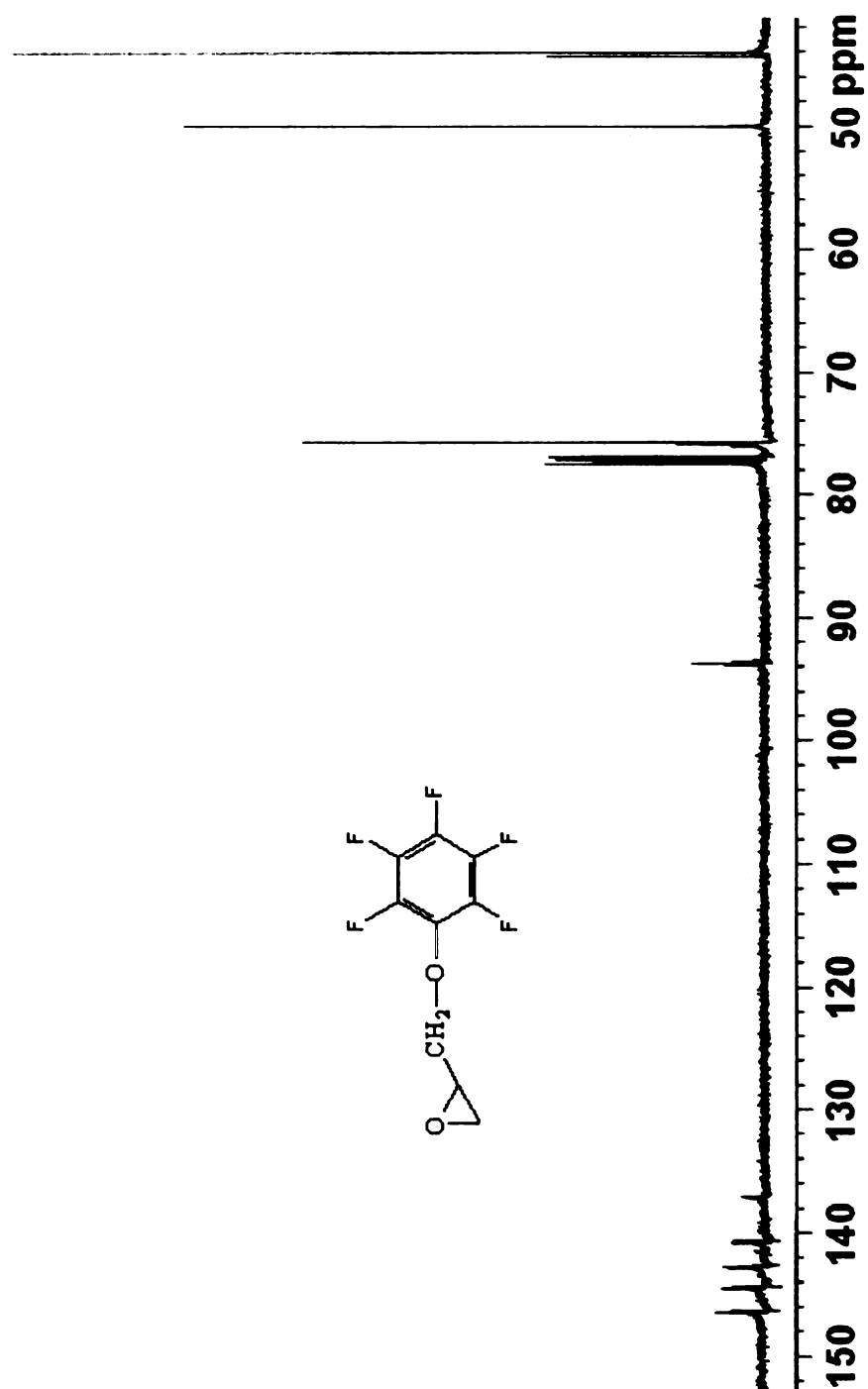
1. H. Araki, A. A. Zakhidov, K. Tada, K. Yakushi, K. Yoshino. *Synthetic Metals* **1996**, 77, 291-297.

## **Appendices**

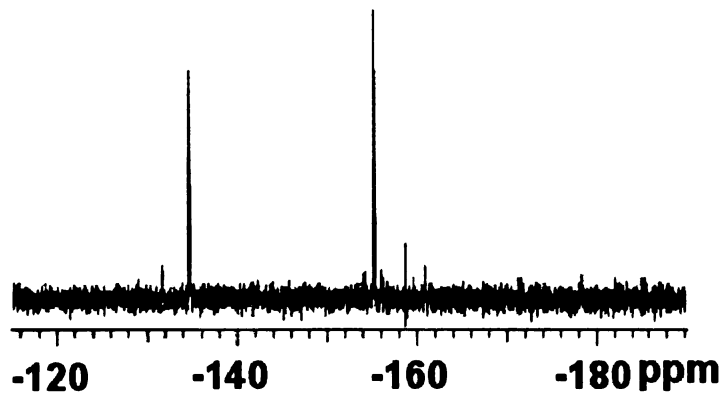
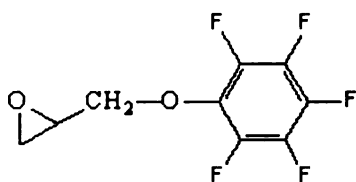




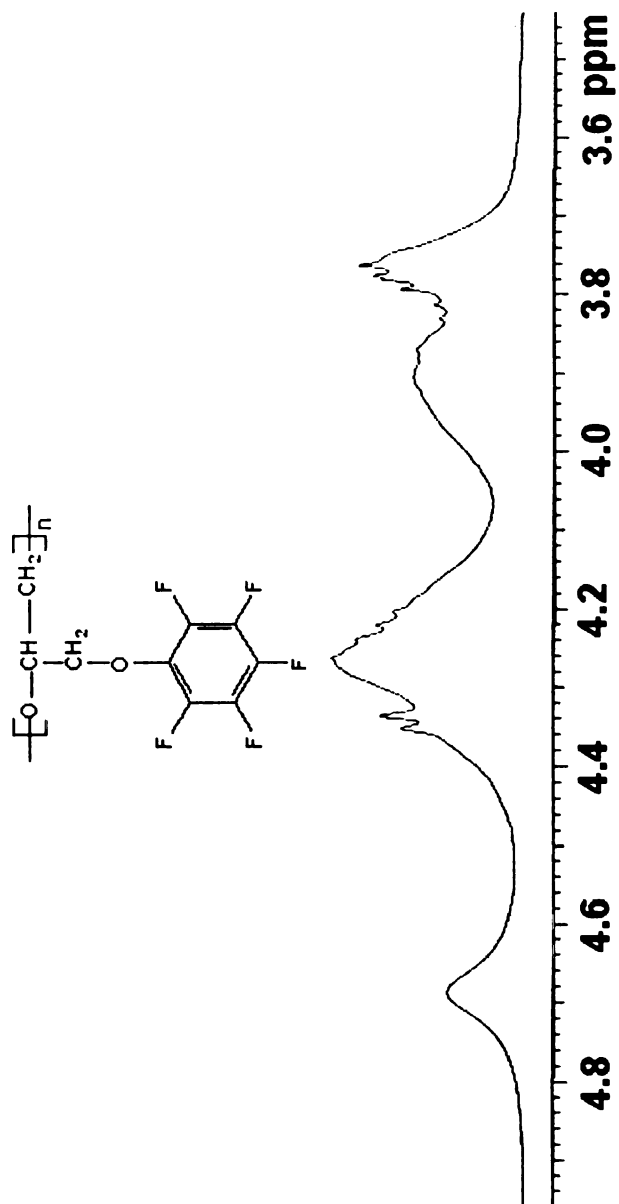
**Appendix 1 -  $^1\text{H}$ -NMR spectrum of glycidyl pentafluorophenyl ether**



**Appendix 2** -  $^{13}\text{C}$ -NMR spectrum of glycidyl pentafluorophenyl ether



**Appendix 3** -  $^{19}\text{F}$ -NMR spectrum of glycidyl pentafluorophenyl ether



**Appendix 4** - <sup>1</sup>H-NMR spectrum of poly(glycidyl pentafluorophenyl ether)

MICHIGAN STATE UNIVERSITY LIBRARIES



3 1293 02470 8699